

2002

Dispersion compensation in fiber optic communication systems

I-Wei Hong
San Jose State University

Follow this and additional works at: https://scholarworks.sjsu.edu/etd_theses

Recommended Citation

Hong, I-Wei, "Dispersion compensation in fiber optic communication systems" (2002). *Master's Theses*. 2319.
DOI: <https://doi.org/10.31979/etd.4x26-5th4>
https://scholarworks.sjsu.edu/etd_theses/2319

This Thesis is brought to you for free and open access by the Master's Theses and Graduate Research at SJSU ScholarWorks. It has been accepted for inclusion in Master's Theses by an authorized administrator of SJSU ScholarWorks. For more information, please contact scholarworks@sjsu.edu.

INFORMATION TO USERS

This manuscript has been reproduced from the microfilm master. UMI films the text directly from the original or copy submitted. Thus, some thesis and dissertation copies are in typewriter face, while others may be from any type of computer printer.

The quality of this reproduction is dependent upon the quality of the copy submitted. Broken or indistinct print, colored or poor quality illustrations and photographs, print bleedthrough, substandard margins, and improper alignment can adversely affect reproduction.

In the unlikely event that the author did not send UMI a complete manuscript and there are missing pages, these will be noted. Also, if unauthorized copyright material had to be removed, a note will indicate the deletion.

Oversize materials (e.g., maps, drawings, charts) are reproduced by sectioning the original, beginning at the upper left-hand corner and continuing from left to right in equal sections with small overlaps.

ProQuest Information and Learning
300 North Zeeb Road, Ann Arbor, MI 48106-1346 USA
800-521-0600

UMI[®]

DISPERSION COMPENSATION IN FIBER OPTIC COMMUNICATION SYSTEMS

A Thesis

Presented to

The Faculty of the Department of Electrical Engineering

San Jose State University

In Partial Fulfillment

of the Requirements for the Degree of

Master of Science

by

I-Wei Hong

August 2002

UMI Number: 1410419

UMI[®]

UMI Microform 1410419

Copyright 2002 by ProQuest Information and Learning Company.
All rights reserved. This microform edition is protected against
unauthorized copying under Title 17, United States Code.

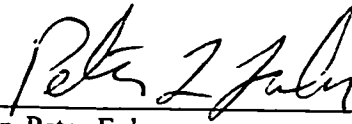
ProQuest Information and Learning Company
300 North Zeeb Road
P.O. Box 1346
Ann Arbor, MI 48106-1346

© 2002

I-Wei Hong

ALL RIGHTS RESERVED

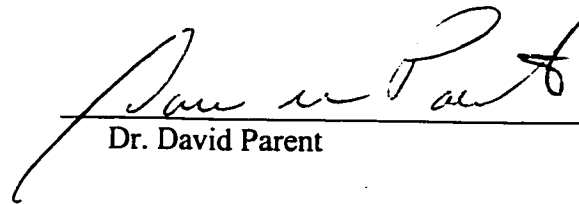
APPROVED FOR THE DEPARTMENT OF ELECTRICAL
ENGINEERING

A handwritten signature in cursive script, appearing to read "Peter Fuhr", written over a horizontal line.

Dr. Peter Fuhr

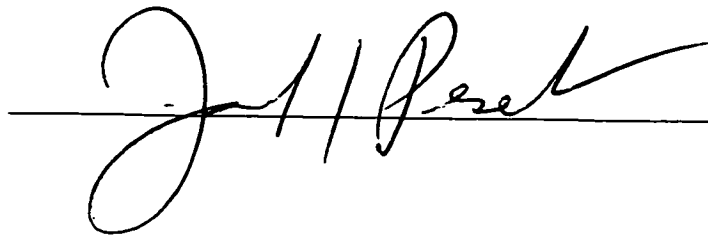
A handwritten signature in cursive script, appearing to read "Sun Chiao", written over a horizontal line.

Dr. Sun Chiao

A handwritten signature in cursive script, appearing to read "David Parent", written over a horizontal line.

Dr. David Parent

APPROVED FOR THE UNIVERSITY

A large handwritten signature in cursive script, appearing to read "J. Parent", written over a horizontal line.

Abstract

As the data transmission rate keeps increasing, the chromatic dispersion causing pulse broadening becomes an important factor of signal degradation in fiber optical networks. Many efforts have been drawn to the development of dispersion compensating devices to recover or prevent the broadening signal pulse. A novel design of tunable dispersion compensating fiber Bragg grating (FBG) device is demonstrated in this paper. This device can provide a dynamically tunable dispersion through an adjustable chirped FBG by physically deformation of the FBG. The theory of operation and experiment result are presented.

ACKNOWLEDGEMENT

First of all, I would like to thank Professor Peter Fuhr for support and guidance. It is always a pleasure to work with him. His wisdom, patience and humor helped me and guided me through all the difficulties to the end. I was truly fortunate to have Peter as my thesis advisor. I really appreciate Professor Sun Chiao and Professor David Parent for their valuable time to review my report in detail.

Most of all, I am grateful to the love and support of my parents and my family. Without their support, I cannot make it here.

TABLE OF CONTENTS

LIST OF FIGURES	VIII
-----------------------	------

LIST OF TABLES	IX
----------------------	----

CHAPTER 1: FIBER OPTIC COMMUNICATION AND COMPONENTS.....	1
--	---

1.1 FIBER OPTICAL COMMUNICATION	1
1.2 OPTICAL FIBERS.....	6
1.3 OPTICAL SOURCES	8
1.3.1 Production Of Light	8
1.3.1.1 SPONTANEOUS EMISSION	9
1.3.1.2 STIMULATED EMISSION	9
1.3.2 Light Emitting Diodes (LEDs).....	10
1.3.2.1 Operation and Construction of LEDs	10
1.3.2.2 General Characteristics of LEDs	13
1.3.3 Laser Diodes (LDs).....	15
1.3.3.1 Semiconductor Laser Diodes	15
1.3.3.2 Fabry Perot Laser Diodes.....	17
1.3.3.3 Single Mode Laser Diodes.....	18
1.4 ERBIUM-DOPED FIBER AMPLIFIER (EDFA)	20
1.5 DIFFRACTION GRATING DEMULTIPLEXER.....	22
1.6 OPTICAL ADD/DROP MULTIPLEXER.....	23
1.7 PHOTODETECTORS	25
1.8 SUMMARY	26

CHAPTER 2: OPTICAL SIGNAL DEGRADATION.....	28
--	----

2.1 OPTICAL SIGNAL ATTENUATION.....	28
2.2 MATERIAL DISPERSION.....	30
2.3 WAVEGUIDE DISPERSION	31
2.4 MODAL DISPERSION	32
2.5 POLARIZATION MODE DISPERSION	33
2.6 DISPERSION COMPENSATION	33
2.6.1 Dispersion Shifted Fiber	34
2.6.2 Non-zero Dispersion Shifted Fiber	35
2.6.3 Dispersion Compensating Fiber.....	36
2.7 SUMMARY.....	36

CHAPTER 3: FIBER BRAGG GRATING.....	38
-------------------------------------	----

3.1 INTRODUCTION TO FIBER BRAGG GRATING	38
3.2 FABRICATING A LONG BRAGG GRATING.....	41
3.3 TYPICAL BRAGG GRATING OPERATION AND CHIRP BRAGG GRATING	43
3.4 DISPERSION COMPENSATION USING CHIRP BRAGG GRATING.....	45
3.5 SUMMARY.....	48

CHAPTER 4: EXPERIMENT AND RESULTS.....	50
4.1 BENDING FIBER BRAGG GRATING	50
4.2 EXPERIMENT CONFIGURATIONS.....	52
4.3 STRAIN RESPONSE MEASUREMENT	56
4.4 TEMPERATURE RESPONSE MEASUREMENT	58
4.5 SUMMARY	60
 CHAPTER 5: CONCLUSION.....	 61
5.1 DISCUSSION OF THE EXPERIMENTAL RESULTS.....	61
5.2 SUGGESTIONS FOR FUTURE RESEARCH.....	62
 REFERENCES.....	 63

LIST OF FIGURES

Figure 1-1 A standard fiber optic communication system-----	2
Figure 1-2 DWDM channels and fiber attenuation curve -----	4
Figure 1-3 (a) Structure of an optical fiber; (b) Cross-sectional view of multimode fiber and single mode fiber -----	7
Figure 1-4 Two major optical fiber types -----	8
Figure 1-5 Energy bandgap and light emission of LED -----	11
Figure 1-6 Surface-emitting (Burros) LED -----	12
Figure 1-7 Edge-emitting LED -----	13
Figure 1-8 Laser Cavity -----	16
Figure 1-9 (a) Index-Guiding Laser Diode; (b) Buried-Heterostructure (BH) Laser Diode -----	17
Figure 1-10 Fabry-Perot Laser -----	17
Figure 1-11 Distributed-feedback (DFB) laser -----	19
Figure 1-12 Distributed Bragg reflector (DBR) laser -----	20
Figure 1-13 Erbium doped fiber amplifier -----	22
Figure 1-14 Diffraction Grating Demultiplexer -----	23
Figure 1-15 Optical Add/Drop Multiplexer -----	24
Figure 1-16 Anatomy of an avalanche photodiode detector (APD) -----	26
Figure 2-1 Rayleigh scattering -----	29
Figure 2-2 Chromatic dispersion -----	31
Figure 3-1 Fiber Bragg grating acts as a wavelength filter -----	39
Figure 3-2 One method of fiber Bragg grating fabrication -----	40
Figure 3-3, A periodic grating in the core of a photosensitive optical fiber by two interfering UV beams of wavelength λ_{UV} -----	41
Figure 3-4 Experimental set-up for writing technique of long fiber Bragg grating -----	42
Figure 3-5 Spectra from a commercially available Bragg grating -----	43
Figure 3-6 Schematic diagram of step-chirped grating -----	44
Figure 3-7 Configuration for writing linearly chirped fiber gratings -----	45
Figure 3-8 Chirped Bragg grating for dispersion compensation -----	47
Figure 4-1 FBG mounted cantilever beam -----	51
Figure 4-2 Photograph of a global view of the experimental setup -----	52
Figure 4-3 Photo of fiber Bragg grating attached cantilever beam -----	54
Figure 4-4 Photo of bended cantilever beam -----	54
Figure 4-5 Experiment arrangement used for measurement of strain response of fiber Bragg grating -----	55
Figure 4-6 Strain response of the FBG at different level of vertical beam displacement -----	57
Figure 4-7 Shift of central reflected wavelength due to beam displacement -----	57
Figure 4-8 Photo of experiment setup for temperature response measurement -----	58
Figure 4-9 Reflected spectra of FBG measured at different temperature -----	59
Figure 4-10 Shift of central reflected wavelength due to temperature variation -----	60

LIST OF TABLE

Table 1-1 Light Emitting Semiconductors----- 11

CHAPTER 1: FIBER OPTIC COMMUNICATION AND COMPONENTS

Communication is an important part of our daily life. Everyday, we are using different types of communication services, such as voice, video, images, and data communication. As needs for those services increase, demands for large transmission capacity networks also increase. In order to fulfill the increasing demand for higher data rate and larger bandwidth, lightwave technology has been developed. The combination of photons and glass fibers provides a tremendous transmission capability improvement compared to transmission lines through electrons and copper wires. As a result, fiber optical transmission systems are now widely deployed in the backbone network. Clearly, fiber optic transmission technology will remain the key communication technology for the foreseeable future.

1.1 FIBER OPTIC COMMUNICATION

The idea of using a glass fiber to transmit information light over long distances was first introduced by Kao and Hockman in 1966 [1]. This was realized when low-loss glass optical fibers were first fabricated by Corning in 1970 [2]; almost the same time, room temperature operating semiconductor diode lasers were developed by Bell Labs [3]. The combination of a compact optical transmission medium and a miniature diode laser produced a series of revolutions in fiber optical communication technology. This technology was adapted by the telecommunication industry starting in the 1970s. Currently, it is widely applied in different types of communication systems, such as Internet and cable TV networks. This is due to the ever-increasing demand for “more data, less time” in transmission of voice, image, video, and so forth. While the end game

into a residence may use twisted pair wire, coaxial cable, or even a wireless architecture, it is optical fiber that is relied on for the primary distribution of the data from location to location.

Consider the situation shown in Figure 1-1, where cable TV and telephone service providers both use a standard fiber optic communication system to deliver their communication services to residences.

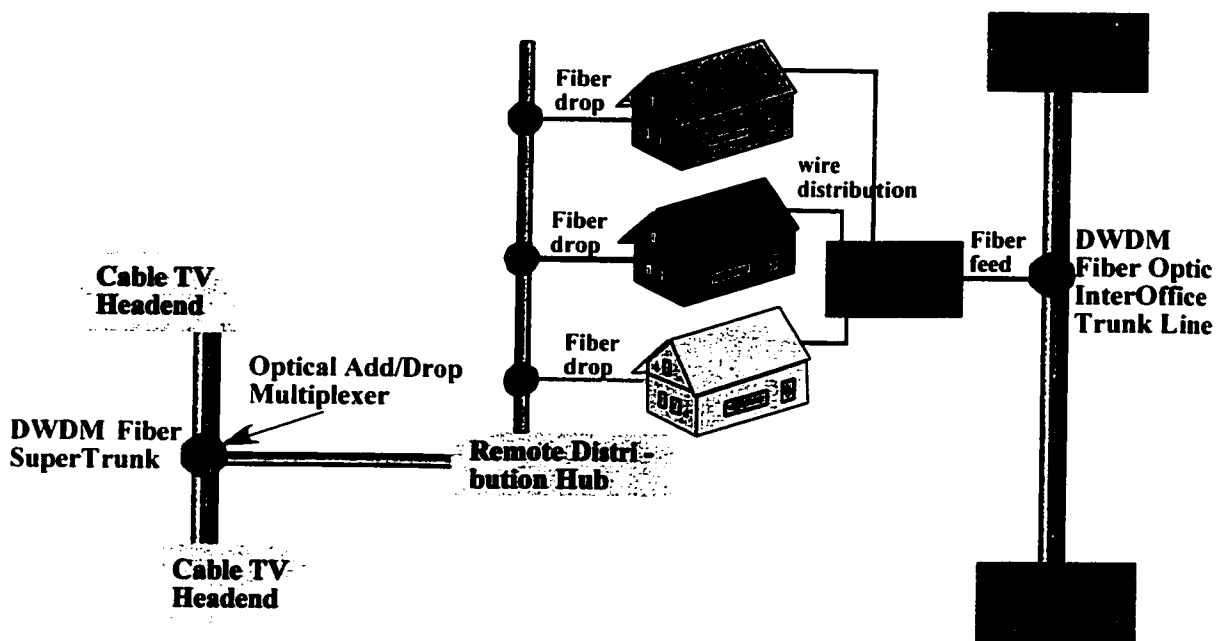


Figure 1-1, A standard fiber optic communication system is exemplified to show how two different communication service providers, e.g., cable TV and telephone companies, use fiber to deliver services

On the television side of the communications system, the cable TV company receives broadcast signals from satellites and terrestrial sources. A single analog TV channel requires ~6 MHz of bandwidth, with 10 MHz typically assigned for each channel. Each cable channel is then placed onto adjacent RF carriers with a frequency separation of 10 MHz. A traditional cable delivery system utilizing coaxial cable will

have an upper frequency limit of approximately 450 MHz (44 channels) [4]. The bandwidth associated with a few TV channels may be allocated for cable modem delivered Internet service. On the other side, the telephone company delivers phone service into the residence via, in most instances, twisted pair wire. In many areas, the phone service may still be strictly analog (~ 4 kHz) while in many urban/suburban areas the service is migrating towards delivery of digital signals - potentially providing some form of digital subscriber loop (xDSL) delivered Internet service. While the lines of services provided may blur, e.g., Internet telephony over cable modems or Internet-based television over xDSL, the guiding idea is simple - provide wider bandwidth channels efficiently and cost-effectively.

Fiber optic communications systems are able to provide wide bandwidth cost effectively. In modern fiber optic communication systems, the dense wavelength division multiplexing (DWDM) technology has been developed to provide ultra-high bandwidth communications [5]. In DWDM architecture, multiple laser sources operating at different λ (or wavelength) are used with each source's wavelength transmitting data at 2.5 Gbps for OC-48 interface or 10Gbps for OC-192 interface. These independent wavelengths are placed very closely together at $0.8 \text{ nm} \approx 100\text{GHz}$ channel spacing in the 1550 nm range (ITU-T G.692 standard), with carrier wavelengths that are tuned to lie within a minimum in the optical fiber's attenuation curve (Figure 1-2) [6].

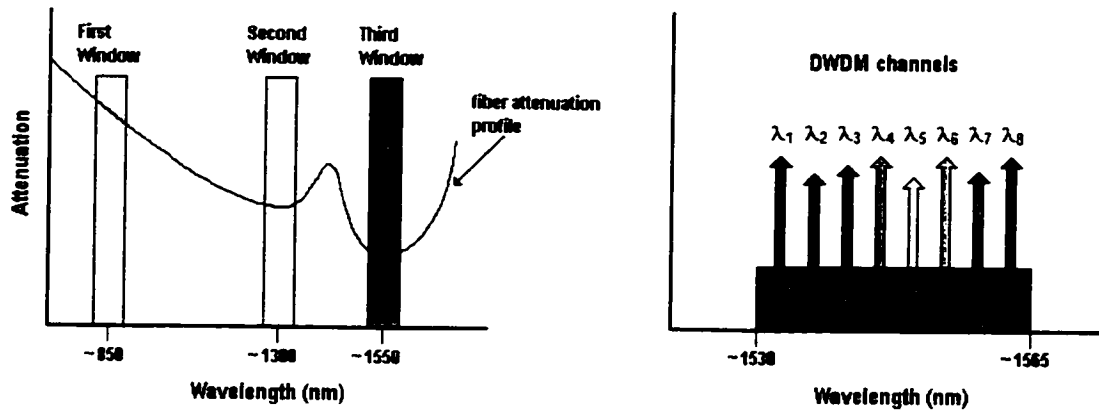


Figure 1-2, The DWDM architecture is predicated on providing wide bandwidth (2 Gbps) laser-based optical communication signals within the so-called "3rd window," the 1530-1565 nm range, of a fiber's attenuation curve

Transmitting multiple signals, such as telephone traffic originating in different area codes, in a Dense Wavelength Division Multiplexing (DWDM) scheme is strikingly similar in structure to the frequency multiplexed scheme used in cable TV's delivery of multiple television channels. In the cable system, different channels are placed onto different carrier frequencies (e.g., cable channel 2, cable channel 3,..., cable channel 41, etc.) resulting in a broadband delivery of multiple channels. In the DWDM case, different collections of data/information are placed onto different optical carrier frequencies, sometimes referred to as wavelengths (λ) or colors, resulting in a broadband delivery of multiple "channels." As an example, consider a fiber network which transports telephone/data traffic in the north California area: DWDM methodologies imply that, area code 408 traffic is placed onto $\lambda_1=1544$ nm, area code 510 traffic is placed onto $\lambda_2=1544.8$ nm, area code 415 onto $\lambda_3=1545.6$ nm, etc.

In a classic wavelength division multiplexing systems (WDM), two data channels were chosen to allow one channel to operate within each of the optical fiber's two inherent attenuation windows, namely 1310 nm and 1550 nm, a DWDM system attempts to pack many more laser wavelengths into each of these windows in the fiber attenuation curve. The tradeoffs associated with each of these fiber windows, e.g., pulse spreading via dispersion, differing levels of signal attenuation, are frequently weighed against the costs associated with having to amplify or even regenerate the signal pulses. In other words, if the overall system loss, due to the length of the fiber and/or the number of taps into the fiber, is low, then perhaps no signal amplification is required. That in turn implies that Erbium-Doped Fiber Amplifiers (EDFAs) won't be used (remembering that they really only work in the 1530-1565 nm range) so we may just as well place the laser signals in the 1300-1320 nm fiber "window" AND the 1530-1565 nm "window." The overall system costs are reduced, principally due to no need for signal amplification. This kind of architecture is so called Metro-DWDM system suitable for ultra-high speed metropolitan or inner-city network applications [7]. Alternatively, if the optical signal must have amplification, then in most instances one or more EDFAs will be used. This then restricts the DWDM operation to the 1530-1565 nm range. Such architecture is so called Long-Haul DWDM system that can provide a high bandwidth optical link for hundreds of kilometers [8].

A modern optical communication link depends mainly on four components: the optical transmitter, the optical receiver, the optical fiber, and the optical amplifier. The optical transmitter is used to generate light signal and modulate information on the signal, the optical receiver receives the transmitted signal and converts it back to the carried

information, the optical fiber is the transmission media of light, and the optical amplifier is used to extend the transmission distance. In dense wavelength division multiplexing (DWDM) systems, in addition to the above four devices, more components are required in order to load or retrieve transmission traffic on different λ (wavelength) [9]. A small core set of components of a DWDM system is introduced in the following sections.

1.2 OPTICAL FIBERS

Optical fiber consists of a very fine cylinder of glass core, through which light propagates. The core is surrounded by another layer of glass, named cladding, which is then wrapped by a thin plastic jacket (See Figure 1-3). The core glass has a slightly higher index of refraction than the cladding glass. The ratio of the refractive indices of core and cladding defines the critical angle θ_c : $\sin\theta_c = n_2/n_1$, where n_1 is the refractive index of the core and n_2 is the refractive index of the cladding. What makes fiber optics work is the total internal reflection: when a ray of light goes from the core to the core-cladding boundary at an angle larger than θ_c , the ray is completely reflected back to the core. Therefore, light signals can be guided inside optical fibers [10].

Optical fibers are typically referred to as either single-mode or multimode with the difference resulting from the larger core diameter in the case of the multimode fiber. The size of the core of a single-mode fiber is usually 9 microns, while the core of a multimode fiber is usually 50 or 62.5 microns. Multimode fibers allow multiple paths, called modes, for the light to travel in them. For single-mode fiber, a smaller core makes it possible to restrict the light propagates in one mode or one path only down the fiber. However, it also depends on the wavelength used. At very long wavelengths, even “multimode” fiber can propagate only a single mode. At short wavelengths, several

modes of light may propagate in a “single-mode” fiber. So single-mode fibers have so called cutoff wavelength. Below the cutoff wavelength, a single-mode fiber becomes multimode [11].

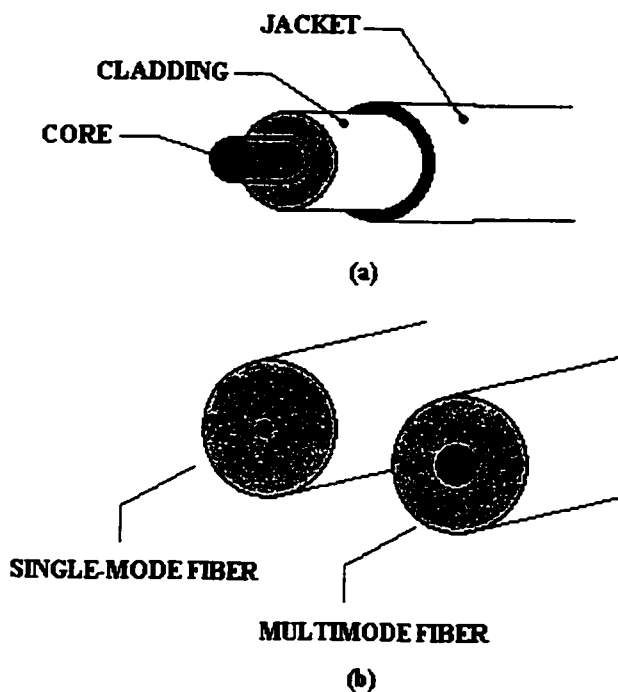


Figure 1-3, (a) Structure of an optical fiber; (b) Cross-sectional view of multimode fiber and single mode fiber.

A quick look at these two types of fiber reveals that more light may be coupled into the multimode fiber (due to its larger core). However, there is typically more signal loss associated with a multimode fiber as well as more signal distortion due to the multiple paths that the light signal may take as it proceeds along this larger fiber. With their smaller core region, single mode fibers provide more spatial control of the optical field resulting in significantly less distortion as well as less signal loss. In either case, the

outside diameters of single-mode and multimode fibers tend to be approximately 125 micrometers (or about the size of a thin strand of hair).

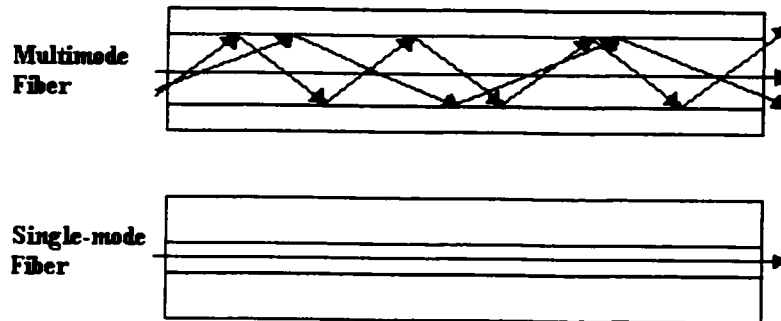


Figure 1-4, Two major optical fiber types

1.3 OPTICAL SOURCES

In the arena of optical communications, an optical source is used to generate an optical frequency carrier, and the carrier is modulated according to the transmitted data and passing through the fiber to the receiver. This section discusses important light sources used in optical communications.

1.3.1 PRODUCTION OF LIGHT

In a general case, there is only one way that light can be produced; if an electron exists in a state of relatively high energy, then rapidly changes to a more stable state (of lower energy), a photon and/or phonon is emitted. Emission of a photon can be spontaneous or stimulated by the passing of another photon of the proper energy [12]. If a phonon is emitted, then the quantum efficiency of that material is usually poor, thus its use will be limited as an optical source.

1.3.1.1 SPONTANEOUS EMISSION

This process is due to an electron reaching an excited state of relatively low stability. The excited electron only remains in this state for mere picoseconds, whereupon it falls to a more stable state releasing a photon. The photon released will have a stochastic phase and direction but its wavelength will be determined by the bandgap energy just traversed. Some substances like a tungsten filament have many energy levels, so upon excitation photons of many wavelengths are emitted, in other words an incoherent light is generated. Spontaneous emission is the process of optical production observed in light emitting diodes (LEDs) and laser diodes (LDs) while below threshold.

1.3.1.2 STIMULATED EMISSION

The major reason why this process can occur is the relative stability of the excited state. Upon excitation an electron can stay in this more stable excited state for microseconds versus picoseconds in spontaneous cases. It is this extra time at the top of the mountain that allows time for a photon of the proper energy to sweep by and stimulate the electron to fall and release a photon. The punch line is that the emitted photon has the exact same phase, direction and wavelength of the photon that stimulated it. So now we have two photons just alike in color, direction and phase, which means the population of signal carrying photons is doubled! For these phenomena to be of use (in say a LASER), we must have population inversion. That is the amount of electrons residing in the excited state must outnumber those in the rest state. Therefore, for coherent light generation, stimulated emission needs to dominate over spontaneous emission.

1.3.2 LIGHT EMITTING DIODES (LEDs)

Virtually all optical sources used in communications today are made from semiconductors. LEDs have a lot in common with laser diodes but are simpler, so the operation and construction of LEDs should be introduced first.

1.3.2.1 OPERATION AND CONSTRUCTION OF LEDs

The most basic LED is a forward biased p-n junction, usually referred to as active layer. If free electrons in the conduction band fall to rest in the ground state (valence band), photons are given off in a 1:1 ratio. The larger the traversed band gap, the shorter the wavelength of emitted light. Refer to the equation below:

$$\lambda = \frac{hc}{E_{\text{photon}}} \quad (1-1)$$

where λ is the wavelength of emitted light, h is Planck's constant, c is the speed of light in vacuum, and E_{photon} is the energy of photon gained by traversing the bandgap. This implies that the material of LED construction determines the emission wavelength. The table below illustrates common LED and laser diode material used [13]. Some materials in the above chart have ranges of wavelengths. This is because different proportions of each element can be mixed, thereby altering the bandgap energies (within reason). Additionally the level of dopant used is important on power and performance as well as wavelength produced. As a general rule the junction area has a relatively large concentration of doping.

Material	Formula	Wavelength Range (μm)	Bandgap Energy
Aluminum Arsenide	AlAs	0.59	2.09
Aluminum Gallium Arsenide	AlGaAs	0.8-0.9	1.4-1.55
Gallium Arsenide	GaAs	0.87	1.42
Gallium Indium Phosphide	GaInP	0.64-0.68	1.82-1.94
Gallium Phosphide	GaP	0.55	2.24
Indium Arsenide	InAs	3.60	0.34
Indium Gallium Arsenide	InGaAs	1.0-1.3	0.95-1.24
Indium Gallium Arsenide Phosphide	InGaAsP	0.9-1.7	0.73-1.35
Indium Phosphide	InP	0.92	1.35

Table 1-1, Light-Emitting Semiconductors

When an electron combines with a hole, one photon is released, so power output is equal to the number of electrons recombined multiplied by the band gap energy, all scaled by an efficiency factor. The recombination of electrons and holes is illustrated in Figure 1-5.

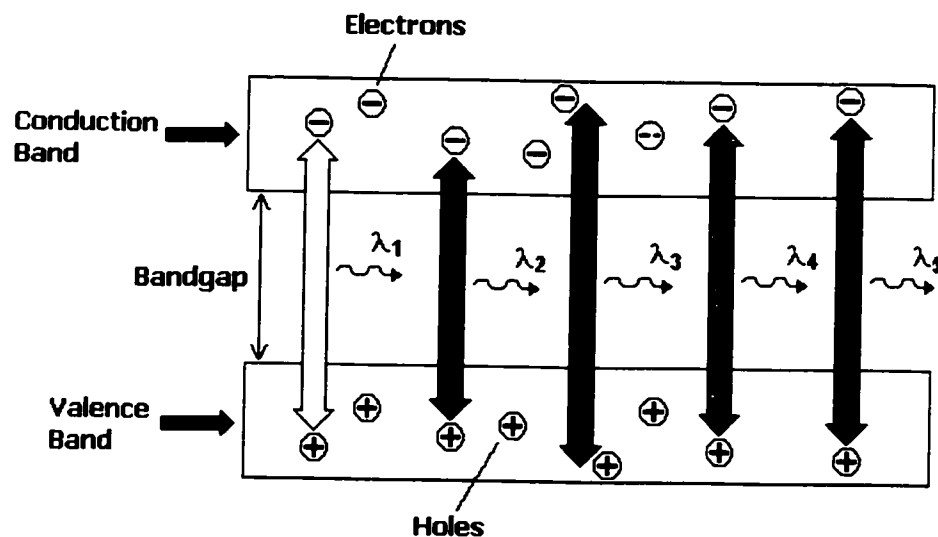


Figure 1-5, Energy bandgap and light emission of LED

In a semiconductor light source, the conduction and valance bands are actually separated energetically. At reasonable temperatures, the majority of holes and electrons lie near the bandgap edges. The double-headed arrows represent a transition between any energy states in the bands. If we use injected carriers (such as in a junction diode) the dominating transition is from the higher potential conduction band down to the subordinate valance band. If on the other hand, energy is pumped into the LED via heat or excitation with light, then electrons can flow in the opposite direction.

Due to the inherent nature of a LED's multiple energy levels, a broad range of wavelength are emitted (or say an incoherent light). A typical LED, like a GaAlAs LED, could have an emitting range in the order of 100nm [14]. The light emitting spectrum width (or say linewidth) also depends on how the emitted light is coupled out of the active layer. There are two different coupling structures for LED: surface emitting [15] and edge emitting, as illustrated in Figures 1-6 and 1-7.

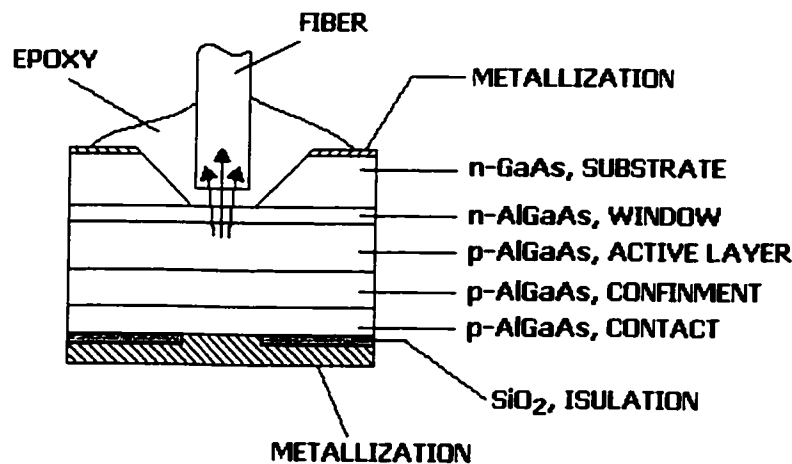


Figure 1-6, Surface-emitting (Burrus) LED

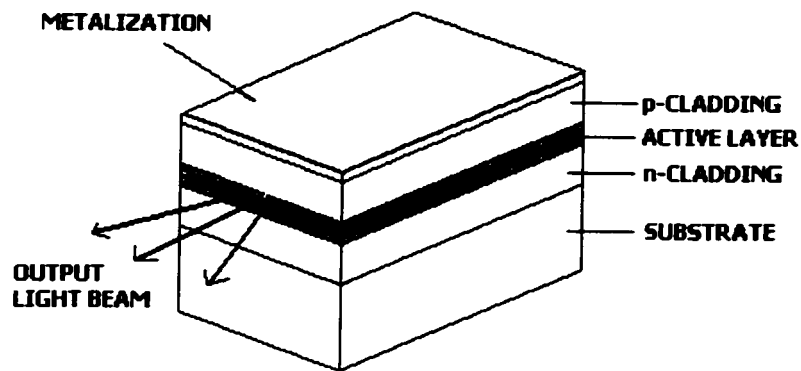


Figure 1-7, Edge-emitting LED

The first type couples light vertically away from the planar emitting surface and is called surface-emitting or Burrus LED. The second type couples light out in parallel to the active layer and is called edge-emitting LED. Because of self-absorption along the length of the active layer, edge-emitting LEDs have smaller linewidth than those of surface-emitting diodes [16].

1.3.2.2 GENERAL CHARACTERISTICS OF LEDs

Relative Low Cost: In the past LEDs were significantly cheaper than their laser diode competitors. At present this has changed significantly. People began using mass-produced lasers from CD-ROM players for multimode fiber communications since 1996. The major sticking point here is that LEDs can't be effectively used in single-mode fibers because of the non-coherence of light and coupling challenges with a $9\mu\text{m}$ core. The coupling inefficiency factor adds a lot of cost to the whole LED idea.

Low Power versus Laser: The maximum optical power of an LED has been typically $100\mu\text{W}$. In the past couple of years major strides have been made in LED technology

leading to LEDs with output power in the 75mW range. This jump in output does make an LED par with a solid state laser for communications. However, other things besides raw power come into play here, as the next bullet will show.

LED's Relatively Wide Emission: LEDs can have a spectral width between 50 to 100nm.

If the signal is coupled directly into the optical pipe, then we have a major case of dispersion for long-haul applications (because with an LED we must use MM fiber and we have a large spectral footprint). However, the spectral width can be reduced via selective filters but this greatly reduces the optical signal, maybe to the point of non-practicality.

Incoherent Output: The light produced from an LED is neither coherent nor directional.

This necessitates a lens to couple light with a fiber. As stated previously, the core of a single mode fiber (9 μ m) is in reality too small to hit with lenses.

Digital Modulation: A direct modulation scheme is usually used to modulate digital signal onto an optical carrier, the output power of LEDs is driven by a signal driving current. When the current switching rate goes higher than LED's 3-dB bandwidth, it's power decreases rapidly. LEDs have a typical modulation bandwidth of 300 MHz. The longer power rise times of LEDs compared to laser diodes, also restrict the use of LEDs in digital systems. Typical LED rise times range from a few nanoseconds to 250ns.

Analogue Modulation: If the forward voltage is maintained above the bandgap energy, the LED can be modulated in an analogue manner (because LEDs respond in a linear fashion with current flow). This is one advantage favoring LEDs; lasers can't be analogue modulated easily, as will be explained in the next section.

1.3.3 LASER DIODEs (LDs)

Another important type of light source use in optical communications is the laser diode (LD). A basic laser diode structure is very similar to that of the edge-emitting LED as shown in Figure 1-7, in a different that an additional confinement structure for transverse photons is added. In virtually all cases from a communication standpoint, lasers are the superior choice over LEDs.

1.3.3.1 SEMICONDUCTOR LASER DIODES

The major difference between a laser and LED lies mostly in the construction. Laser diodes can be monolithically integrated with other optical components; this reduces overall cost and can increase coupling efficiency. Semiconductor lasers are constructed via a planar method, by building several thin layers of material under controlled conditions and doping on top of an InP substrate. Sandwiched between the n- and p-type layers of InP (cladding), is the active layer. This region could be composed of say, InGaAsP. When a bias current is applied, the holes and electrons in the active region reach a state of excitation. When they recombine (mostly by stimulation), energy is released in the form of a photon. Wavelength is dependent on the active region's band-gap, just as it was in an LED. The active region has a much higher refractive index than

does the cladding making it act as a semiconductor waveguide, so light is mostly confined to the active region. However, the two lateral sides of the laser diode also need additional confinement structures to reduce the cavity loss as shown in Figure 1-8.

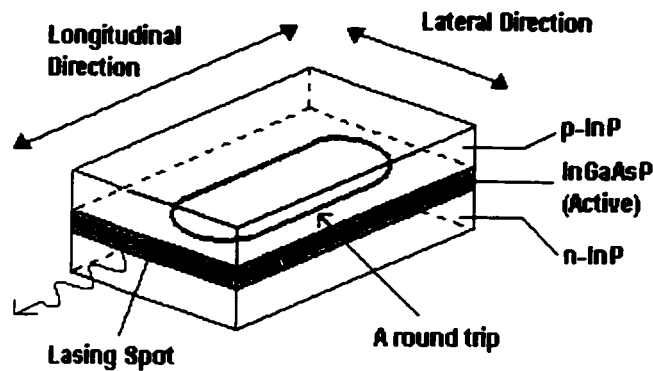


Figure 1-8, Laser Cavity

Several cavity confinement techniques have been developed to improve the power efficiency of laser diodes [17,18]. For example, an extra waveguide layer can be grown above or below the active layer, this provides an index change at the two lateral sides and helps confine the emitted light, which is called index-guided laser (Figure 1-9(a)). Even more aggressively, two more heterojunctions can be added to the lateral sides to force light moves inside a narrow strip along the length of the laser, which is called buried-heterostructure (BH) laser (Figure 1-9(b)).

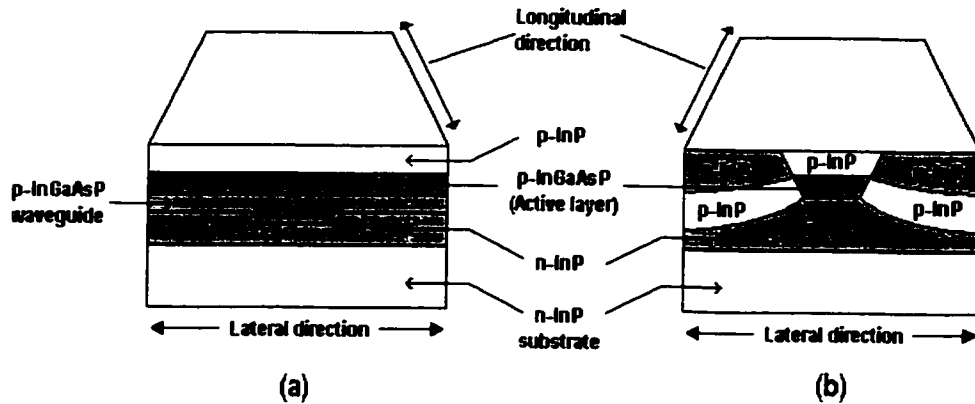


Figure 1-9, (a) Index-Guiding Laser Diode; (b) Buried-Heterostructure (BH) Laser Diode

Semiconductor lasers transmit a beam coherently in a narrow cone, so light is more easily coupled into a single mode fiber. Additionally, they can be modulated directly at rates to 10Gbps without optical chirping.

1.3.3.2 FABRY-PEROT LASER DIODES

Basically a Fabry-Perot laser is just an LED with two monolithic mirrors. The purpose of the mirrors is to provide an environment for lasing to occur. The laser is so named because its cavity acts as a Fabry-Perot (Etalon) filter. The diagram below depicts a basic Fabry-Perot filter design.

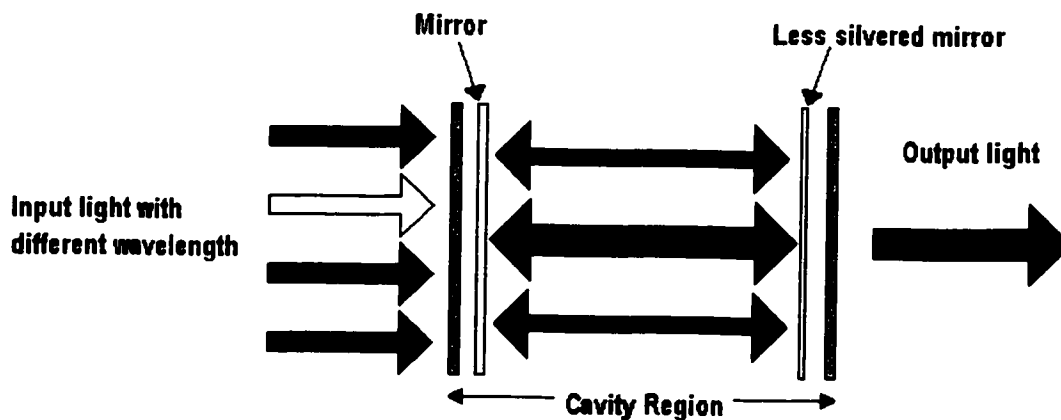


Figure 1-10, Fabry-Perot Laser

Light enters through the partially silvered mirror on the left and indirectly exits through the less silvered mirror on the right. Only wavelengths that resonate within the cavity are allowed to pass through. The other wavelengths cancel each other out destructively. In a LASER, the cavity would be composed of a material that would provide coherent gain for the dominant (resonant) wavelength, thus outputting a relatively pure color with increased power. Only when the distance between mirrors is an integral multiple of $1/2$ wavelength, will the light reinforce itself. Destructive interference cancels out other wavelengths. This principle only holds true if the cavity length is on the order of 400 wavelengths or less. Devices have been constructed with an active region of 30 wavelengths. The drawback here is reduced gain, the smaller the active region, the less material you have to reach a state of population inversion. The following formula relates intra-mirror distance to wavelength.

$$L = \frac{m\lambda}{2n} \quad (1-2)$$

where L is the length of the cavity, λ is the output wavelength, n is the refractive index of the cavity, and m is an arbitrary integer.

1.3.3.3 SINGLE MODE LASER DIODES

For high-speed long-distance communications a single mode laser is required, which generates only one main longitudinal mode. Consequently the spectral width of the output light is very narrow, so the carried signals have a better immunity to dispersion caused pulse spreading.

One way to generate only a single longitudinal mode is to reduce the length L of the lasing cavity of a Fabry-Perot laser to the point where the separation of the adjacent

modes given in Equation 1-2 is larger than the laser transition line width, only a single longitudinal mode is allowed to resonate within the small cavity. However, this means the length of FP cavity should be reduced to about 25 μm or smaller and the output power has mere few milliwatts [19]. The extra small size and low output power limit the utility of FP single-mode lasers in practical applications.

A different kind of laser called distributed-feedback (DFB) lasers use a built-in frequency-selective structure to suppress undesired modes. As illustrated in Figure 1-11, there is a periodic structure inside the laser cavity with the period equal to Λ . Because of this periodic structure, a forwarding traveling light has interference with a backward traveling light. As a result, a constructive interference only occurs at a wavelength that is a multiple of the period Λ . This is called the Bragg diffraction, which is described as:

$$\lambda_B = \frac{2n_e \Lambda}{m} \quad (1-3)$$

where λ_B is the resonant wavelength called Bragg wavelength, Λ is the periodic spacing, n_e is the effective refractive index, and m is an integer presenting the order of the grating. The first order ($m=1$) provides the strongest output power. Therefore the period of the periodic structure determines the wavelength of the single-mode light output.

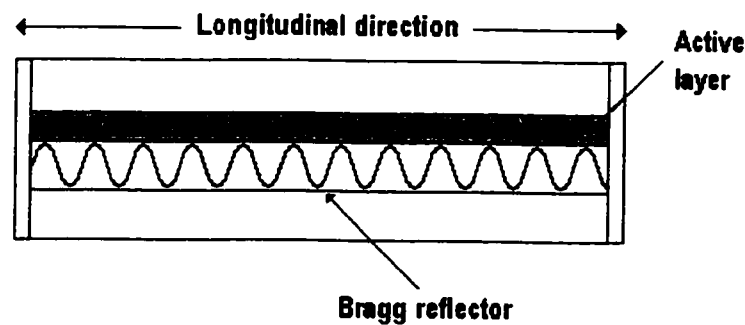


Figure 1-11, Distributed-feedback (DFB) laser

Alternatively, the Bragg diffraction structure can be built outside the laser cavity instead in the cavity as DFB lasers. This kind of structure is used in distributed Bragg reflector (DBR) lasers as shown in the Figure below.

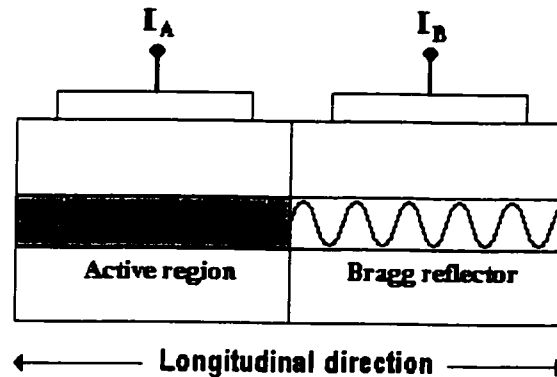


Figure 1-12, Distributed Bragg reflector (DBR) laser

The advantage of this arrangement is that the power control (laser cavity) and the wavelength control (Bragg reflection cavity) can be done separately. For applications such as wavelength division multiplexing (WDM) and frequency division multiplexing (FDM), tunable lasers based on DBR laser have been developed to provide selectivity of output wavelength (or say frequency) [20]. In general, the output wavelength can be electrically tuned by adjusting the bias current of the Bragg reflector.

1.4 ERBIUM DOPED FIBER AMPLIFIERS (EDFAs)

The first demonstration of optical amplification within rare earth doped optical fiber was reported in 1964 [21]. Optical excitation of the Erbium occurs by injecting photons with wavelengths corresponding to Erbium absorption peaks into the Erbium doped fiber. Electrons within the Erbium crystal are elevated into metastable states by

using a pumping light source at wavelength 980nm or 1480nm. Amplification occurs due to the fact that when photons with wavelengths in the 1550nm range encounter this "elevated" Erbium section of fiber, they cause stimulated emission of these elevated states.

For optimal inline optical amplification, the data sequence lie within the 1540-1565 nm range. Even with this restriction on "allowable" wavelengths, Erbium does not provide uniform amplification [22]. However, it does provide its highest levels of amplification efficiency. Inline amplification is performed using an arrangement shown in Figure 1-13: amplification relies on single-mode (SM) fiber, a 2x2 optical coupler (a WDM), a length of Erbium-doped fiber (which has been fusion spliced onto the SM fiber), and an optoisolator (useful but not absolutely required). The Erbium pump signal is injected into one side of the 2x2 couple while the input data sequence is on the other side. On the output side of the 2x2 coupler, both wavelengths propagate within the fiber. Typically one output from the WDM is either terminated or simply illuminates a photodetector (providing a convenient measure of the power). The pump + data signal propagating down the other coupler output enters into the Erbium-doped section of fiber. The pump beam excites the Erbium while the data signal causes amplification through stimulated emission. In certain cases, an optical isolator is then used to prevent any backscattered light, from farther down the SM fiber, to enter back into the Erbium-doped fiber. For a 10m section of Erbium-doped fiber, a pump wavelength of 980 nm will provide approximately 2.2 dB/mW of amplification. Overall amplification saturates around 25 dB.

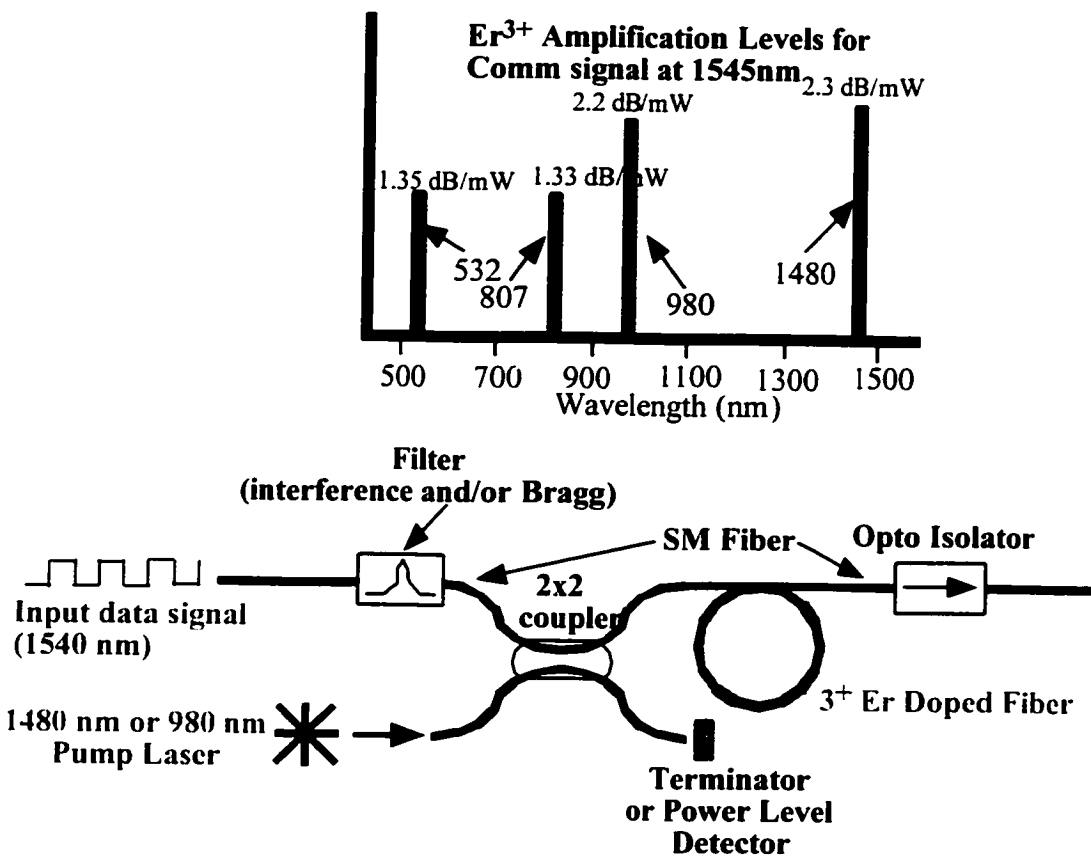


Figure 1-13, While Erbium can provide amplification using a number of pumping wavelengths, the 980 and 1480 nm wavelengths are optimal. In reality, inline amplification is achieved using the system architecture shown.

1.5 DIFFRACTION GRATING DEMULTIPLEXER

Once all of these wavelengths are packed into a single fiber, the job falls to a demodulator to first separate the wavelengths. While there are various methods of performing this task, a conventional diffraction grating may also be used.

In the context of using a diffraction grating as a wavelength filter (or separator) within a fiber optic communication system: Consider the case where two colors, λ_1 and λ_2 are propagating down one single-mode optical fiber. The grating equation, $m\lambda = d\sin\theta$ dictates that for fixed integer m and a fixed grating spacing d , the two colors must exit the

grating at different angles, e.g. θ_1 and θ_2 . By placing single-mode fibers at these angles, the colors will each propagate down their respective output fiber. In essence, a wavelength filter (or a demultiplexer) has just been described. By reversing the direction, this component may also be used as a wavelength combiner - directing, in this case, two wavelengths into a single fiber. Note that this "redirection" capability of a diffraction grating causes, among other things, a net decrease in the signal strength.

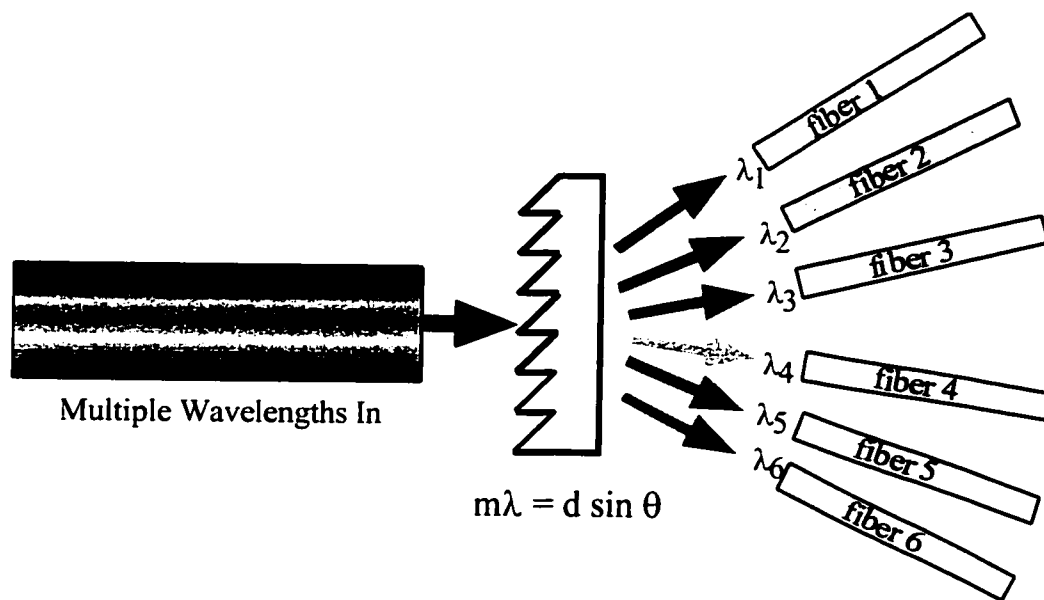


Figure 1-14, A conventional diffraction grating may be used to separate the wavelengths propagating down a DWDM fiber.

1.6 OPTICAL ADD/DROP MULTIPLEXER

The capability to add and or drop traffic from a communication stream is paramount to being able to upgrade or even provide service to customers. Within the DWDM regime, a particularly useful Optical Add/Drop Multiplexer (OADM) scheme uses circulators and gratings. It enables carriers to reroute traffic to different geographic areas without extensive termination equipment. All wavelengths are presented to port 1

of the first circulator. In the dropout portion, all wavelengths (information channels) then exit the circulator at port 2. However, a fiber grating has been spliced into the fiber connecting the two circulators. This grating has special characteristics that allow it to transmit λ_1 (and perhaps 3,4,5,...,n) while λ_2 is reflected. λ_2 then reenters circulator #1, continues around the circle, and exits the circulator #1 at port 3. As a result, a wavelength (or communications channel) has been extracted from the main information artery. Meanwhile, the other wavelengths proceed on to enter circulator #2 at its second port (port 2). These wavelengths just continue around the circle and exit at port 3. Meanwhile, another communication channel data is being carried once again by λ_2 . This signal is injected into port 1 of circulator #2. It exits the circle via port 2, but once again this wavelength encounters the fiber grating and is reflected. The λ_2 lightwave then goes back into circulator #2's port 2, continues a bit of the way around the circle and emerges at port 3, just like the other wavelengths. A wavelength (or communications channel) has been added to the main information artery!

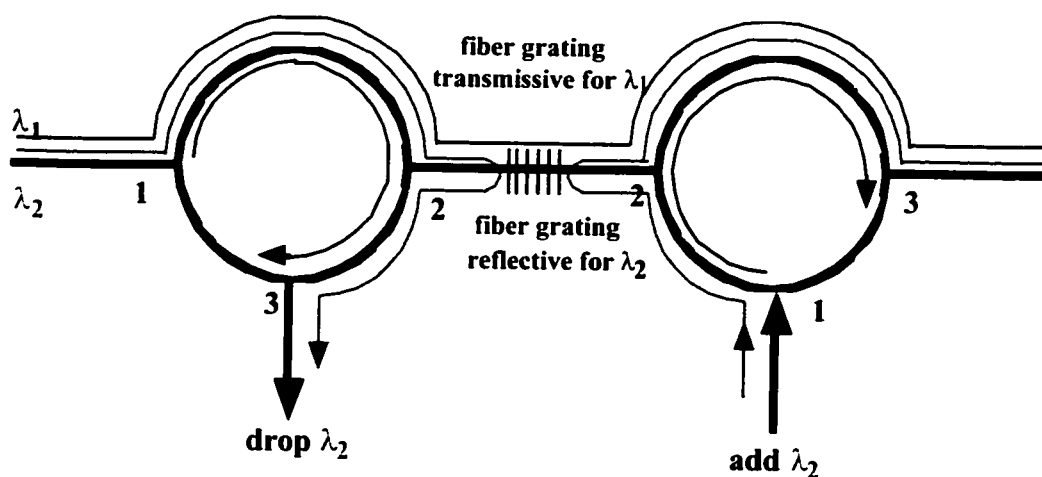


Figure 1-15, An Optical Add/Drop Multiplexer based on Bragg gratings and circulators resembles consecutive rotaries.

1.7 PHOTODETECTORS

The majority of optical detectors used in communications rely on the principle of ionization in a semiconductor material [23]. In other words, for a suitable material, a photon with enough energy (i.e., of the correct wavelength) will strike the surface of the semiconductor, be absorbed and eject an electron. In a conventional PIN diode detector, this photoelectron rapidly migrates to an electrical contact where it is swept out of the detector and most probably electrically amplified. For a frequency response in the GHz range, this implies that a very low amount of stray capacitance can exist within the photodetector itself, which in turn implies that the detector is very small ($\sim 100\text{ }\mu\text{m}$ in diameter). A high-speed transimpedance amplifier boosts the photoelectron signal to a level such that a 0/1 decision may be made. Another frequently used photodetector is an avalanche photodiode detector (APD) - shown in Figure 1-15. While the photoelectron generation principle is essentially the same as with the PIN, an APD provides intrinsic gain thereby reducing the need for an additional transimpedance amplifier. But like most things in life you don't get something for nothing - for with the intrinsic gain comes a need for an $\sim 200\text{V}$ (essentially no current) power supply bias AND, more importantly, noisier performance. Detailed reviews of these photodiodes have been presented in the literature [24-28].

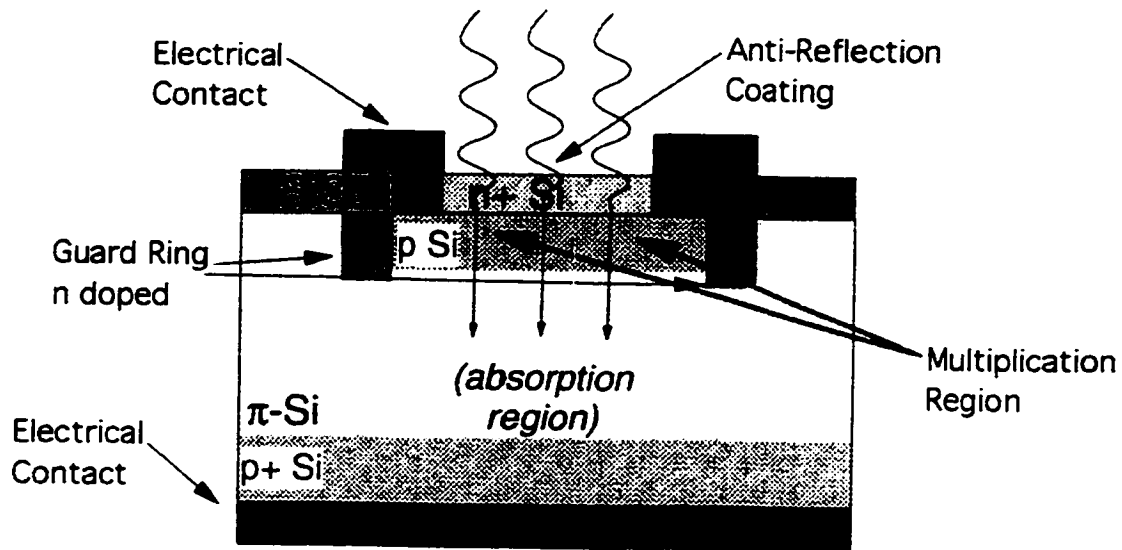


Figure 1-16, Anatomy of an avalanche photodiode detector (APD).

1.8 SUMMARY

Because of the maturing of fiber optic technology, communication networks have been gradually updated with the search for more advanced techniques to take full advantage of the transmission potential of a fiber link. Techniques like wavelength division multiplexing, optical amplifiers, optical switchers, and the management of dispersion enable us to load more transmission traffic on to a single glass fiber. However, the pursuing after speed and bandwidth never stopped.

In order to keep pace with the increasing demand of communication bandwidth, and provide the service cost efficiently, engineers have turned to the development of higher speed TDM and more channel DWDM systems for longer distance. While the power attenuation task is overcome by the invention of optical amplifiers, dispersion causing pulse spreading become the dominant limit of transmission speed and distance of optical communications. As the transmission rate goes from OC-48 (2.5 Gbps) to OC-192

(10Gbps) or even OC-768 (40Gbps), the dispersion compensation requirement will only become more critical for system performance. Although the DCF can generate a negative dispersion to compensate dispersion accumulated in the fiber link, it only provides a partial solution to the dynamically changing dispersion situation. A better solution able to provide tunable dispersion compensation is highly demanded for advanced fiber optic communications. It is the objective of this research project to demonstrate a novel tunable dispersion-compensating scheme based on bending a fiber Bragg grating (FBG) attached cantilever beam.

The fundamental components of a modern fiber optic communication system are described in this chapter. The mechanisms and effect of dispersion and conventional dispersion management are explained in the Chapter 2. The fiber Bragg grating technology, which is important for tunable dispersion compensation solutions, is examined in detail in the Chapter 3. The proposed FBG tuning scheme and experimental results are presented in Chapter 4, and this report is end with a conclusion in the Chapter 5.

CHAPTER 2: OPTICAL SIGNAL DEGRADATION

As an optical signal pulse traveling inside a fiber, there are several factors that can degrade the data transmission. The longer distance an optical pulse goes the less chance the data can get to the receiver end; the faster a pulse is being transmitted the worse the information can be recognized successfully. These are due to the attenuation and dispersion of a propagating lightwave. The attenuation effect decreases the signal power and the dispersion effect distorts the shape of the pulse as a lightwave propagating down a fiber. The mechanisms causing these effects are discussed in this chapter.

2.1 OPTICAL SIGNAL ATTENUATION

Signal attenuation [29] is a very important property in the design of a fiber optical communication system, because it largely determines the maximum transmission distance between a transmitter and a receiver. There are three basic mechanisms causing signal attenuation in a fiber; they are absorption, scattering, and imperfection losses of the optical energy [30-32].

Absorption loss can be classified as two types: intrinsic absorption and extrinsic absorption. The intrinsic absorption is due to the material nature of absorbing specific wavelength regions of light. The intrinsic absorption occurs in both the infrared and ultraviolet ranges. Fortunately, these intrinsic losses are mostly insignificant in the region where fiber systems are operated, but these losses limit the extension of fiber optic communication toward the ultraviolet as well as toward longer wavelength. Extrinsic absorption is caused by the atomic resonance of impurity particles in the fiber. The most important extrinsic absorption is due to water or the hydroxyl ion (OH) bond. Because the bond can absorb incident light at its resonant frequency and harmonics, there are

absorption peaks at wavelengths of $2.8/(n+1) \mu\text{m}$. For example, the first, second, and third overtones of absorption peaks are at 1.40, 0.93, and $0.70 \mu\text{m}$ ($n=1,2,\text{and } 3$) [33,34].

There are four kinds of scattering loss in optical fibers: Rayleigh, Mie, Brillouin, and Raman scattering [35]. Rayleigh is the most important scattering loss. During the manufacture process of glass fibers, some localized variations in density may happen due to random motion of molecular. These material density variations may be modeled as small scattering objects embedded in an otherwise homogeneous material. Because these objects are much smaller than the operating wavelengths, when a beam of light passing through these objects, some of its energy is scattered and lost. The scattering-loss dependence is indicated in Fig. The Rayleigh scattering loss can be approximated by the expression:

$$L = 1.7 \left(\frac{0.85}{\lambda} \right)^4 \quad (2-1)$$

where λ is in micrometers and the loss L is in dB/km [36]. As a result, the scattering loss is proportional to λ^{-4} . Therefore, the use of short wavelength in fiber optic communication is severely restricted by Rayleigh scattering.

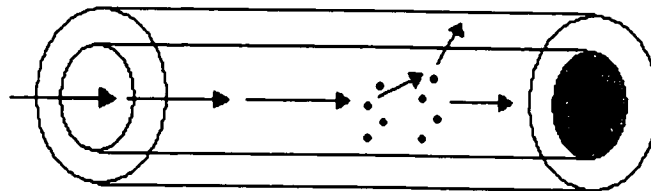


Figure 2-1, Rayleigh scattering, showing attenuation of an incident stream of photons owing to localized variations in refractive index.

The imperfection loss includes bending, coupling, and splicing losses. Bending loss occurs whenever an optical fiber undergoes a bend of finite radius of curvature. When a fiber is bent, partial energy radiates away through the evanescent field tail in the cladding. Generally, bending loss is not significant and can be neglected, unless the bending curvature is too large or higher than the order of 1 mm^{-1} [37]. Usually, a light signal is also attenuated at a junction of two connected fibers either by a coupler or splicing. The loss is caused by some extrinsic or intrinsic reasons. Extrinsic reasons include misalignment, tilt, end gap, or bad end face quality. Intrinsic reasons are core ellipticity, mismatch in refractive index, or mismatch in mode field diameter. Typically, coupling loss is around 0.2 dB and splicing loss is around 0.05 dB [38].

2.2 MATERIAL DISPERSION

As well known, when a light wave travels in a vacuum, it moves at a velocity of $c = 3 \times 10^8 \text{ m/s}$. In any other medium, light waves travel at a slower speed, given by $v = c / n$, where n is the index of refraction of the medium. For the material used to make an optical fiber, the refractive index varies with the wavelength of light traveling inside the fiber. Therefore, a different wavelength (or say color) of light travels at a different speed inside a fiber. The term “dispersion” is used to describe the phenomenon of wavelength dependent velocity of propagation of an electromagnetic wave. When the velocity variation is caused by some property of the material, the effect is called material dispersion.

The material dispersion effect can be explained by considering the situation showed in Figure 1-9. A finite linewidth optical source emits a pulse into a dispersive glass fiber. For simplicity, assume the input pulse is composed by three different single

wavelengths: λ_1 , λ_2 , and λ_3 . The three pure color components travel at different velocities (due to wavelength dependent refractive index) in the fiber. After propagating a distance, they arrived at different time in the receiver end. As a result, the output pulse, the sum of three received single wavelengths, becomes spreading. In a long enough fiber span the dispersion can be sufficiently large so that the adjacent pulses will overlap eventually, this results in inter-symbol-interference (ISI) and producing a high bit error rate in communications.

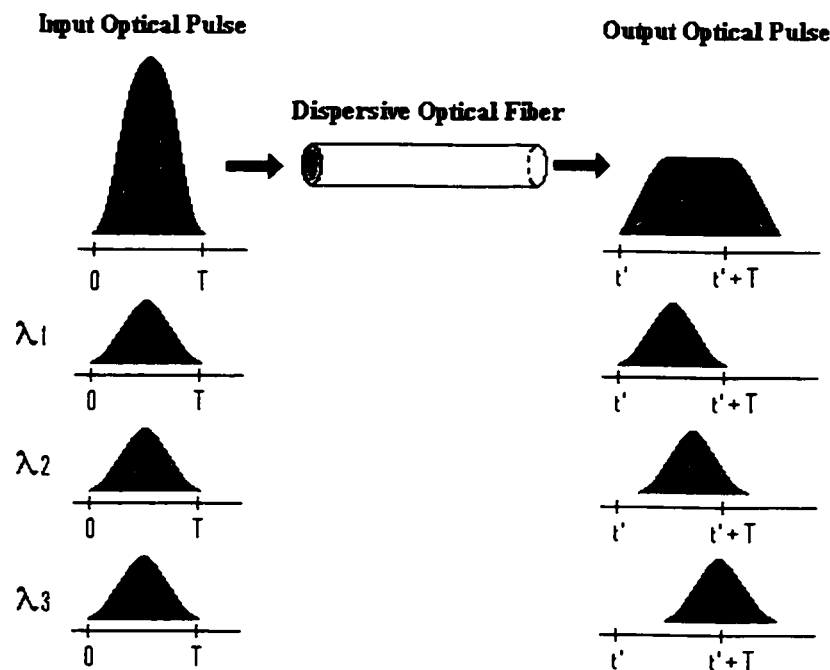


Figure 2-2, Pulse spreading caused by propagation through a dispersive optical waveguide. The complete pulse contains wavelengths λ_1 , λ_2 , and λ_3 ; each has different speed due to wavelength dependent indices of refraction.

2.3 WAVEGUIDE DISPERSION

Another basic type of dispersion is called waveguide dispersion, which is usually ignored in multimode fiber applications. When a light signal is coupled into a single-

mode fiber, only about 80 percent of power is confined into the core, and the other 20 percent of power propagates in the cladding layer [39]. Since the core and cladding have different refractive indices, the two modes of light travel at different speeds. Since the light travels faster in the lower refractive index materials and slower in higher refractive index materials, the light propagating in cladding travels faster than the light confined in the core. Dispersion is then produced. The amount of waveguide dispersion depends on the design of fiber. Waveguide dispersion is a function of the core radius, the refractive index difference between core and cladding, and the shape of the refractive index profile. In fact, the waveguide dispersion can be carefully designed to cancel out the material dispersion at particular wavelength in single-mode fiber design. The resulting optical fibers are known as dispersion-shifted fibers [40-43].

2.4 MODAL DISPERSION

Modal dispersion is a problem only when a multimode fiber is used. Multimode fibers allow different paths or modes for the light to travel in them. The various modes intend to interact with each other in the big fibers. Since different modes propagate at different angles, each of them has a different axial group velocity along the fiber [44]. In other words, they travel at different speeds. This variation in the group velocities of the different modes results in a group delay spread or inter-modal distortion. The modal dispersion limits the speed and distance of an optical communication link. However, this dispersion mechanism can be eliminated when a single-mode fiber is used. That is why some form of single-mode fiber is always used in systems needing the highest speeds and longest spanning.

2.5 POLARIZATION MODE DISPERSION

Polarization mode dispersion (PMD) describes a situation in which the electromagnetic wave components that make up an optical signal travel at different speeds within the fiber. This causes a multipath interference at the receiver. PMD is difficult to predict and may possibly vary with temperature and environment, the twisting of the cable as it was pulled, and even between production runs from the same manufacturer. The very high-speed systems that are soon to be deployed (i.e., 10 Gbps OC-192) are more prone to failing in the presence of significant levels of PMD.

Some modeling has been performed recently that suggests that PMD will only be a problem for long haul systems (i.e., > 500 km). The analysis took into account that link components such as dispersion shifted fiber (DCF) and EDFAs contribute their own degree of PMD. In addition, Corning Incorporated has performed field tests on various vintages of installed Corning fiber and is confident that its standard single-mode product (SMF-28) has a low enough PMD such that it will support OC-192 on existing routes. Keep in mind that existing routes are limited to distances requiring regenerators rather than the cascaded EDFAs those long haul carriers plan to deploy to maximize bandwidth and economize on signal regeneration. Bell Atlantic has been working with Bellcore to examine the embedded fiber for PMD problems; however, it may not pose any practical difficulty until long haul WDM systems are constructed.

2.6 DISPERSION COMPENSATION

As described in previous section, attenuation and dispersion effects can significantly limit the bit rate and the spanning distance of fiber optical communication.

The war against attenuation can be won because the improvement of fiber manufacturing and the invention of EDFA. However, dispersion effects have to be taken into consideration as well. Since PMD is rarely observed, modal dispersion is taken care of by using single-mode fiber, and waveguide dispersion can be controlled by fiber design, it is the material dispersion usually referred to as the main factor of limitation of optical networks. In this section, several important fiber technologies used to provide dispersion compensation are described.

2.6.1 DISPERSION SHIFTED FIBER

The standard single-mode fiber deployed today is manufactured to optimize transmission at 1310 nm by effectively eliminating dispersion at that wavelength. The dispersion in the 1550 nm window far exceeds that for 1310 nm on standard fiber and hence is a limiting factor in single channel or DWDM systems operating in that window. Dispersion shifted fiber (DSF) differs from standard fiber in that the zero dispersion point is shifted from 1310 nm to 1550 nm by constructing a single-mode fiber with a triangular-shaped refractive index variation (instead of a step-index or graded-index variation) [45]. It is best suited for applications involving single channel transmission at 1550 nm providing the benefits of zero dispersion as well as taking advantage of the lower attenuation occurring at that wavelength. WDM systems do not perform as well as single channel systems on DSF due to a phenomenon known as four-wave mixing. Because a fiber's refractive index is nonlinear, two or more optical carriers can combine and produce several mixing products. This has a cascading effect and can result in unwanted products occurring at the operating carrier wavelengths. This process is more

intense when there is zero dispersion at the operating wavelengths because the unwanted products will be moving at the same speed (i.e., in phase) with the desired signals causing significant interference and thereby hampering system performance. There have been some successes with techniques that involve wavelength allocations that avoid mixing products occurring at the signal wavelengths; however, four-wave mixing remains a concern for WDM using DSF.

2.6.2 NON-ZERO DISPERSION SHIFTED FIBER

In order to support WDM systems, a fiber was developed that lowered the chromatic dispersion at 1550 nm but not to the extent that would encourage four-wave mixing as DSF does. This fiber is called Non-Zero Dispersion Shifted Fiber (NZDSF) because of the small non-zero amount of dispersion that occurs in the 1550 nm window. By now it may be apparent that there exists a sort of "Catch-22" situation with TDM and WDM systems. A large telecommunications provider desires to maximize the TDM rates placed on as many WDM optical carriers as possible to maximize the bandwidth of fiber optic facilities. Very high speed TDM requires zero dispersion; however, WDM or DWDM requires some small amount of dispersion to avoid mixing effects. One philosophy is that by a careful combination of NZDSF and standard single-mode fiber in the same link, the benefits of local non-zero dispersion for WDM are realized while also achieving zero dispersion for the total link so that very high TDM rates are possible.

2.6.3 DISPERSION COMPENSATING FIBER

Another philosophy is to use standard single-mode fibers in combination with a new type of fiber. DCF (dispersion compensating fiber) is a new specialty fiber that has a very

high negative value of dispersion [46]. It can actually reverse the effects of chromatic dispersion suffered by 1550 nm signals that traverse standard single-mode fiber. It is used as a sort of inline pre- or post-equalization in the form of a fiber spool of a particular length placed at one end of a link. However, DCF is not an optimal dispersion compensating solution for DWDM systems, because it is efficient for only single wavelength. For a DCF integrated DWDM system, channels located farther from the central wavelength of the DCF get less compensating amount than channels located near the central wavelength. Another disadvantage of DCF is that it cannot handle high optical power due to its relative small effective area. In DCF designs, an increased negative dispersion is achieved by shrinking the core diameter of the fiber. A fiber with a small core diameter experiences high light intensity, or high power per unit area, and, consequently, a system utilizes the fiber will suffer a high level of non-linear effects. Because DCF's high non-linear penalties, its optical power tolerance is limited.

2.7 SUMMARY

To meet growing demand for bandwidth at the lowest possible cost, long haul carriers are migrating to next generation optical networks characterized by high channel counts of 200 or more, high bit rates of 10 Gbps or 40 Gbps, and link distances of thousands of kilometers. Chromatic dispersion has emerged as a key obstacle for system designers in the path to the next generation optical network. The ideal solution should be able to correct dispersion at different wavelength (different channel in DWDM system) and provide continuous flexibility to accommodate network changes and upgrades (for example, migrating from 8 to 16 channels). There are two main technologies providing

channelized dispersion management: fiber Bragg gratings (FBG) and virtually imaged phase array (VIPA), and the FBG based solution is what this research focus on.

CHAPTER 3: FIBER BRAGG GRATING

As mentioned previously, the fiber Bragg grating (FBG), which is widely used in wavelength filtering [47] and smart sensing devices [48], has become a very important technique for doing tunable dispersion compensators. In this chapter, the operational principle of a fiber Bragg grating is first explained, and the fabrication method is then described. In order to understand the operation of FBG in dispersion compensation, different FBG based designs of dispersion compensator are introduced, and the principle of using of FBG to provide dispersion compensation is also explained.

3.1 INTRODUCTION TO FIBER BRAGG GRATING

Fiber grating is a section of fiber with a periodic variation in the refractive index of its core as shown in Figure 3-1. Bragg diffraction effect occurs when an input wavelength equal to one-half of the repetition period Λ goes through the grating region. In the grating region, each change of index of refraction acts like a semi-reflection mirror, and only beams with the selected wavelength ($\Lambda/2$) are reflected and all the reflected beams add up in phase with each other. The reflected wavelength must satisfies the Bragg's law, which is

$$\Lambda = n \frac{\lambda}{2} \quad (3-1)$$

where Λ is the grating period (distance between change of refractive index), λ is the wavelength reflected, and m is the order of the Bragg diffraction. Usually, only the strongest reflection meaning the first order ($n=1$) reflection is taken into account. Alternatively, the phenomenon can be explained as the grating is only resonant at the wavelength obeys Bragg's law.

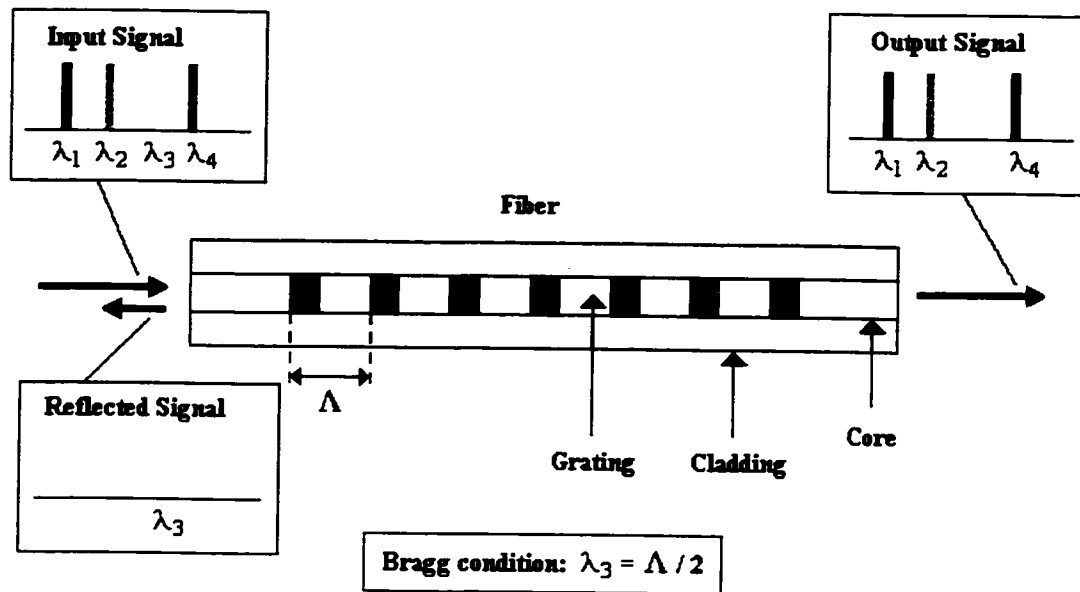


Figure 3-1, Fiber Bragg grating acts as a wavelength filter

The beams at other wavelengths not satisfying Bragg's law are not affected at all, and they pass through the grating region all the way. Therefore, the fiber Bragg grating can be used as an optical filter to block selected wavelength of light signal. This is very attractive for WDM applications. Actually, there have been many researches of optical filter based on FBG [49-51]. This wavelength selective resonance property is also used in the fabrication of narrow linewidth laser diodes.

The grating is formed within the single mode fiber through the inscription of a periodic variation, or modulation, of the fiber core's index of refraction via any of a number of methods. For example, the pattern may be "written" into the core through the use of interfering high power beams as shown in Figure 3-2. Fabrication of the grating is achieved through exposure of the core. Frequently this requires the removal of the fiber's coating layer (such as polyimide), exposure of the core to a very bright light field such as

ultraviolet light, then recoating the fiber with polyimide to restore its durability. The coating removal, exposure and coating reapplication typically reduces the fiber's inherent structural strength by at least a factor of 4 [52]. The end result is effectively a tuned optical filter. The FBG's tuning range is roughly 400-2000 nm with a typical bandwidth of 0.1 nm in the 1300 nm band [53]. Such devices are commercially available from a variety of vendors.

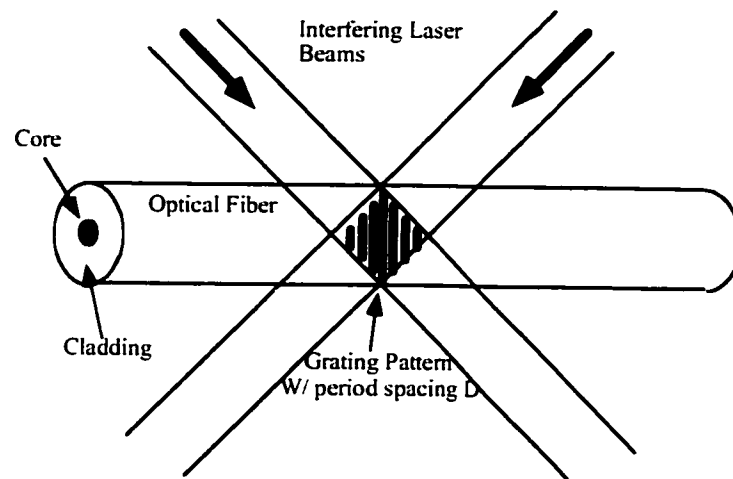


Figure 3-2, One method of fiber Bragg grating fabrication relies on illumination of the fiber by a high intensity interference pattern

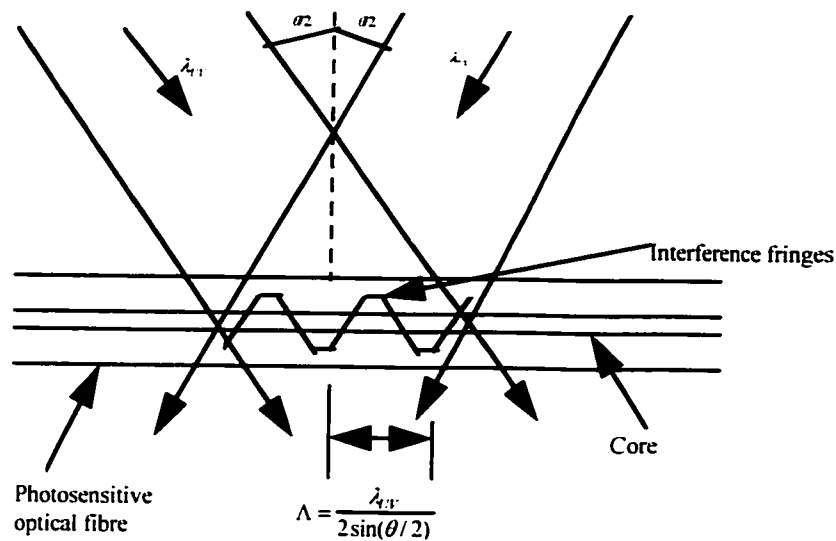


Figure 3-3, A periodic grating in the core of a photosensitive optical fiber by two interfering UV beams of wavelength λ_{UV}

3.2 FABRICATING A LONG BRAGG GRATING

All writing techniques of fiber Bragg gratings, which have been described above, are limited by the size of the writing beam or phase mask. This results in the gratings' physical length to be on the order of mm. An alternative approach would be to have a physically longer grating thereby relaxing some of the constraints present merely due to the conventional grating's small size. Writing long gratings requires a large beam magnification, which causes alignment problems because the UV line focused on the core must be perfectly aligned with the fiber axis. A configuration that has been used for long-grating fabrication, shown in Figure 3-4, is [54] a variation of the phase mask technique that takes advantage of the insensitivity of the phase of the fringe pattern to the beam position.

In this configuration, the fiber is placed directly behind a nulled-zero-order phasemask, and carefully adjusted to be perpendicular to the mask lines. The fiber and mask are held together, and this assembly is mounted on a translation stage.

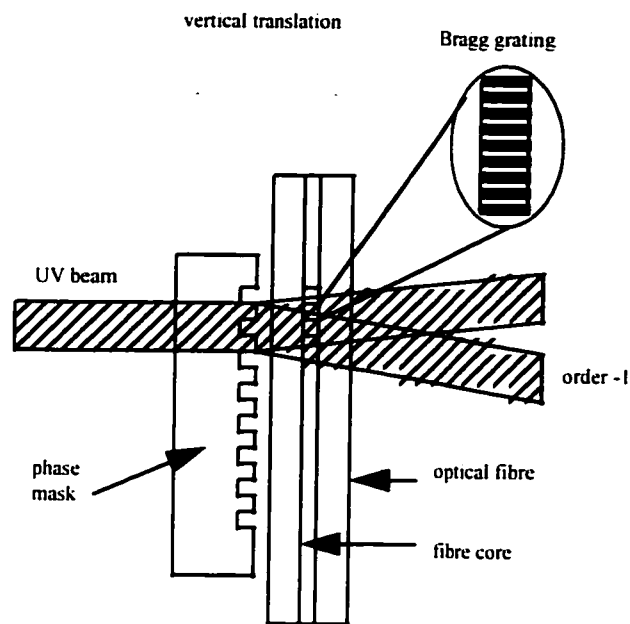


Figure 3-4, Experimental set-up for writing technique of long fiber Bragg grating

By translating the mask-fiber assembly in the direction of the fiber axis, long fiber gratings could be written, limited only by the useful aperture of the mask. The advantage of this technique is that the writing intensity, and thus the grating strength, can be modified along the grating. The phase mask of much larger dimensions can be fabricated relatively easily, using for example electron beam lithography. There is no serious obstacle to the writing of multi-centimeter-long gratings that will find applications for dispersion compensators and ultra-narrow-band filters.

3.3 TYPICAL BRAGG GRATING OPERATION AND CHIRP BRAGG GRATING

The conventional short or long-length fiber Bragg grating may be thought of as a narrow bandpass optical filter. The filter characteristics may be varied through external perturbations interacting with the grating that cause a change in the grating spacing and

therefore the filter's peak wavelength and bandwidth. A typical spectrum from a commercially available grating is shown in Figure 3-5.

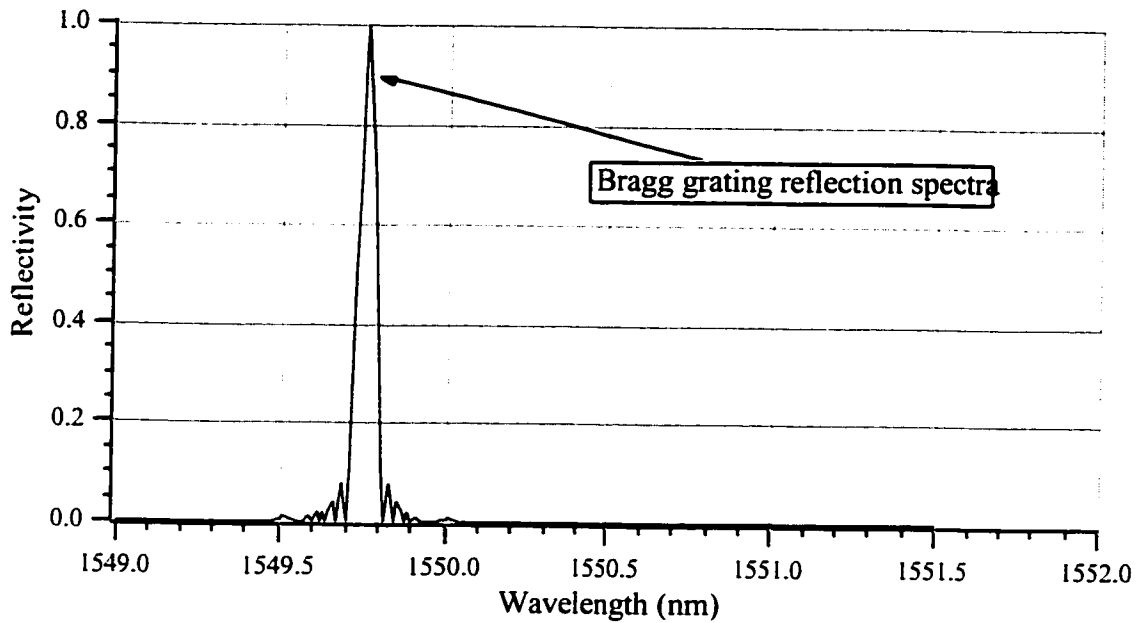


Figure 3-5, Spectra from a commercially available Bragg grating

In most diffraction grating applications, it is desirable to have an effectively no variation in the grating spacing (the Rowland engine used for grating fabrication in the 1800's was legendary for its removal of "diffraction ghosts" which were caused by slight changes in the spacing). However, there are certain instances when the presence of a controlled, linear variation, or chirp, in the spacing, and the accompanying variation in the filter's transmission characteristics may be useful [55].

A chirped fiber Bragg grating may be fabricated using one of a number of methods, with each method realizing a grating of slightly differing chirp parameters. A step-chirp grating is illustrated in Figure 3-6.

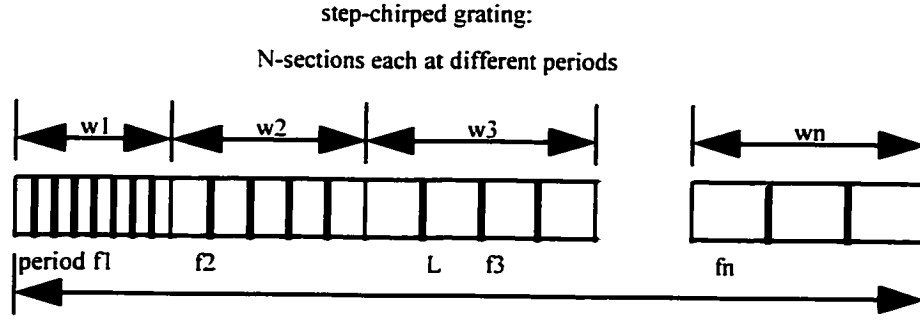


Figure 3-6, Schematic diagram of step-chirped grating

Using the configuration presented in Figure 3-7, a linearly chirped fiber Bragg grating is obtained with its period $p(x)$ given by the following expression [56]:

$$p(x) = \frac{\Lambda}{2} \left(1 - x \left(\frac{\alpha}{f - d} \right) \right) \left(1 - \lambda^2 / \Lambda^2 \right)^{-1/2} \quad (3-2)$$

where Λ is the period of a phase mask; α is the angle between the fiber and the phase mask; f is the focal length of the lens; d is the distance between the lens and the phase mask, and λ is the wavelength of a plane wave. The increase in bandwidth because of the presence of the chirp in a grating of length L is given by

$$\Delta\lambda_c = \frac{nL\Lambda\alpha}{|f - d|\sqrt{1 - \lambda^2 / \Lambda^2}} \quad (3-3)$$

where n is the refractive index of the fiber.

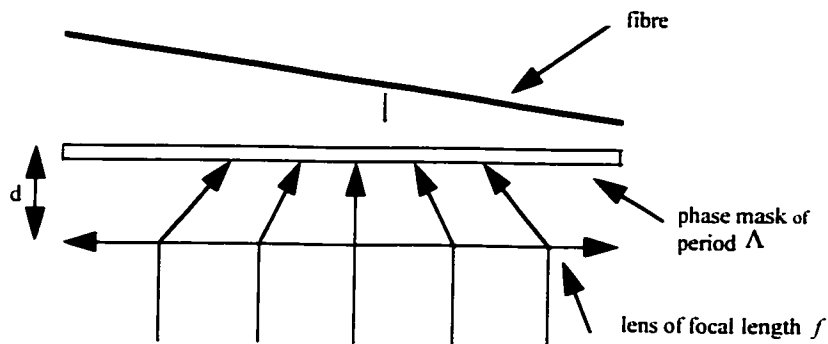


Figure 3-7, Configuration for writing linearly chirped fiber gratings

Many other techniques for the fabrication of chirped Bragg gratings have been reported, such as Byron and Rourke have demonstrated a method for producing chirped fiber Bragg gratings with a uniform period phase mask through a simple stretch and write technique [57]; or tuning and chirping fiber gratings by etching fibers down to very small cladding diameters, so that the propagating modes are affected by the surrounding media [58]; or the technique for fabricating all fiber photo induced chirped gratings by using a step-chirp phase-mask is presented by Kashyap and his co-workers [59] (resulting in the grating index profile shown in Figure 3-6). In each of these fabrication methods, as well as in many other reported techniques [60-63], a "true" chirped period in the fiber's refractive index profile is generated.

3.4 DISPERSION COMPENSATION USING CHIRPED FIBER BRAGG GRATING

The idea of using linearly chirped optical fiber Bragg gratings as linear wavelength dependent reflectors in order to compensate chromatic dispersion was first proposed by Ouellette et al. [64]. A chirped Bragg grating can be used to provide dispersion compensation through the reflections of different wavelengths at different locations that results a compensating time delay reverse to the dispersive delay from the

fiber link. This effect is illustrated in Figure 3-8. Let us consider a pulse that has been broadened because of accumulated dispersion after traveling a long fiber link. For the light at 1.55 μm , because of the negative material dispersion slope, longer wavelength components have a smaller group velocity and hence move slower than short wavelengths [65]. As the pulse propagates, these slower components separate from the faster and shorter wavelength components. This results in pulse spreading. Let us consider two wavelength components of a broadened pulse: the shortest one (λ_s) is at the leading edge of the pulse, and the longest one (λ_l) is at the trailing edge, as illustrated in Figure 3-8. In other words, $\lambda_l - \lambda_s = \Delta\lambda$, where $\Delta\lambda$ is the source spectral width. All wavelengths between λ_l and λ_s will arrive after λ_s and before λ_l . In the chirped fiber Bragg grating, the component λ_s is reflected at the farther end, while the component λ_l is reflected at the near end. At the reflection output, the two components will have a relative delay of

$$\tau = 2 \frac{L_g}{v_g} \quad (3-4)$$

where v_g is the group velocity of the pulse and L_g is the distance between the reflection locations of each components [66]. This delay can be adjusted to be equal, but have opposite sign, to the delay accumulated during the propagation along the fiber link. The broadened pulse is then compressed by the filtering of the chirped Bragg grating, and the dispersion is compensated.

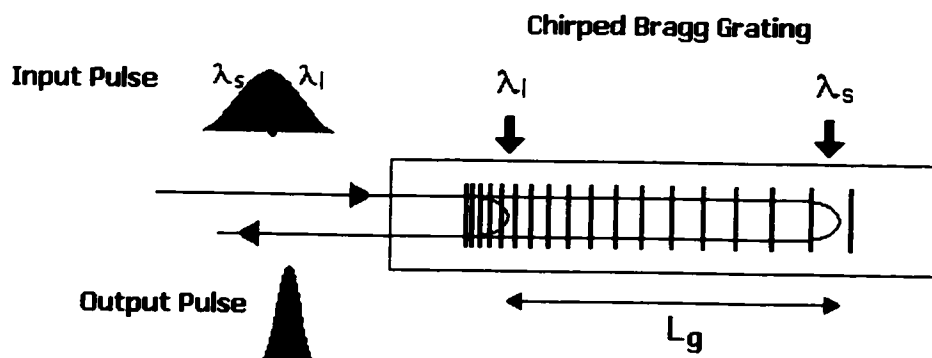


Figure 3-8, Chirped Bragg grating for dispersion compensation

For dispersion compensating applications, chirped Bragg gratings are usually built on a uniform period in-fiber Bragg grating. This is due to the inherent low insertion loss and the allowance for tuning ability of fiber Bragg grating. Typically, there are two major parameters used to “tune” a fiber Bragg grating into chirp: strain and temperature. Many research groups have proposed different techniques for dispersion compensation based on either strain [67-69] or temperature [70-73] control of FBG. In these devices, a strain gradient or a temperature gradient is applied on a uniform FBG to form a chirping variation of the grating spacing and the effective refractive index. Thus, a dynamically tunable dispersion can be provided through the variation of the applied gradient (strain or temperature) profile along the FBG.

Different mechanisms are used to control the strain gradient or temperature gradient. For strain tuning devices, a tunable strain gradient can be produced by simply gluing a FBG on a fixed base and pulling it as proposed by Hill and Eggleton [67], or a more accurate tuning method by using a segmented piezoelectric stack with individually voltage controlled segment used to control local strain along the grating [68]. For temperature tuning devices, a FBG is mounted in a thermally conductive plate (usually

within a V-groove), and the each end of the plate is connected to a heater and a heat sink. A temperature gradient is established on the supporting plate and a similar gradient is induced in the FBG [70-72]; a more compact design can be done by coating the FBG with a thin film of metal to provide the temperature gradient [73]. The variation in the reflective Bragg wavelength caused by strain and temperature fluctuations can be described in terms of the photo-elastic and thermo-optic effects [74] as

$$\Delta\lambda_B = 2n\Lambda \left\langle \left\{ 1 - \left(\frac{n^2}{2} \right) [p_{12} - \nu(p_{11} + p_{12})] \right\} \Delta\varepsilon + \left\{ \alpha + \frac{(\partial n / \partial T)}{n} \right\} \Delta T \right\rangle \quad (3-5)$$

where Λ is the grating period, n is the effective index of the fiber core, p_{ij} are the Pockel's coefficients of the stress-optic tensor, ν is the Poisson's ratio, α is the coefficient of thermal expansion of the fiber material, ΔT is the temperature change and $\Delta\varepsilon$ is the strain variation. The factor $\{(n^2/2)[p_{12} - \nu(p_{11} + p_{12})]\}$ is known as the photo-elastic coefficient. Using bulk values for the strain-optic coefficients and low levels of germanium doping in the core, the photo-elastic coefficient is approximately equal to 0.22. The resultant theoretical wavelength shift caused by strain variation is approximately 1 pm/ $\mu\varepsilon$ at a wavelength of 1300 nm. The wavelength strain sensitivity of a 1550nm Bragg grating is 1.15 pm/ $\mu\varepsilon$ while its temperature sensitivity is 13 pm/ $^{\circ}\text{C}$ [75].

3.5 SUMMARY

As mentioned earlier, the effect of chromatic dispersion becomes more and more critical at high data rate transmission, because the linear dispersion tolerance decreases with the square of the bit rate [76]. Many fiber-Bragg-grating based dispersion-compensating solutions have been proposed to cancel the accumulated dispersions in

fiber links due to the low insertion loss and great tunable range of in-fiber gratings. Tunable ability of dispersion compensator becomes an important feature for multi-wavelength systems, because different wavelength channels can acquire different amounts of dispersion and nonlinear phase shift [77]. For FBG devices, dynamically tunable dispersion is achieved by chirping the grating based on either strain-dependent or temperature-dependent wavelength shift effect. A novel FBG strain tuning scheme based on a bending cantilever beam will be demonstrated in the next chapter.

The role of dispersion compensator will become increasingly important as fiber link distances and data rates increase. Apparently, the compact, low insertion loss and tuning flexible FBG will still be the chosen technology to implement tunable dispersion management in the near future.

CHAPTER 4: EXPERIMENT AND RESULTS

The conventional short- or long- length fiber Bragg grating acts like a narrow bandstop optical filter. The filter characteristics can be changed through external perturbations (e.g. strain and temperature) interacting with the grating. These strain and temperature dependent effects have been referred to the photo-elastic and thermo-optic effects and have been explained in chapter 3. By utilizing the photo-elastic effect, a strain-based dispersion-tuning scheme can be achieved by bending a fiber Bragg grating attached cantilever beam. In order to demonstrate the idea of tuning dispersion range by physically bending a fiber Bragg grating, an experiment is setup to measure the response of a fiber Bragg grating respect to variations of strain and temperature.

4.1 BENDING FIBER BRAGG GRATING

A uniform spacing fiber Bragg grating can be transformed to a grating with variable spacing by attaching it to a mechanical element that undergoes a nonlinear change of shape. For example, LeBlanc et al [78] demonstrated Bragg grating chirping through a simple strain of a fiber that was rigidly attached to a cantilever beam of a non-uniform cross-section. Let us consider a configuration with a beam with physical length of L , the beam thickness t and its width b (see Figure 4-1). Applying a force F at the deflector point ($x = l$) creates a strain distribution in the beam. By using the pure bending theory [79], the axial component of strain is given by

$$\varepsilon(x) = 12 \frac{F(l-x)v(x)}{E_{af}b(x)t^3(x)} \quad (4-1)$$

where E_{af} is Young's modulus of the material, $b(x)$ is the beam width, $t(x)$ represents the beam's thickness and $v(x)$ is the distance from the midplane.

Strain or stress in beams exists because they are subjected to loads that act laterally on the longitudinal axis. Lateral loads acting on a beam cause the beam to bend, thereby deforming the axis of the beam into a curve. Before the load is applied, the longitudinal axis of the beam is a straight line. After loading, the axis is bent into a curve that is called the deflection curve of the beam. For pure bending, it refers to flexure of a beam under a constant bending moment, which means that the shear force is zero.

In practice, F is not known but is an increasing function of deflection. By increasing the deflection with an increasing F , both the average strain and the geometry-determined gradient in the beam are increased. In this experiment, the beam geometry determines the shape of the strain profile and the beam deflection determines the magnitude of the gradient and the average wavelength shift of the reflection spectrum.

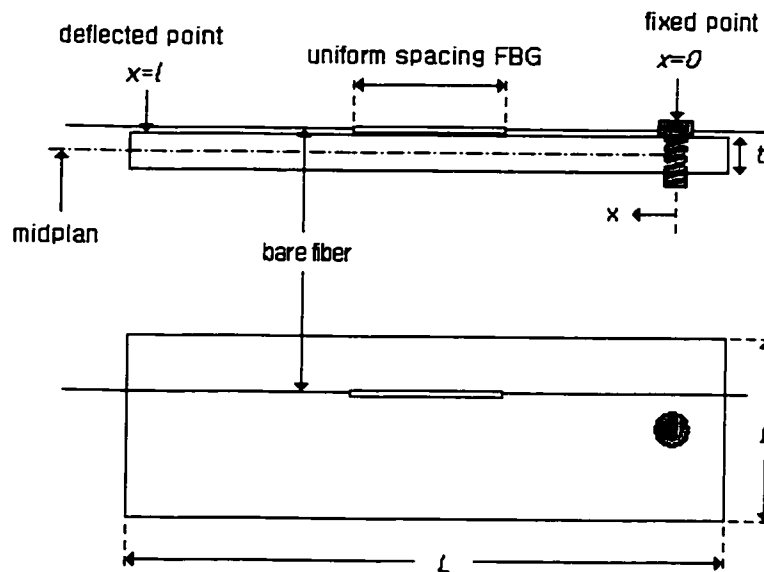


Figure 4-1, FBG mounted cantilever beam

A uniform spacing fiber optic Bragg grating was bonded onto a rectangular beam, which was bended to produce a linear strain variation. The strain dependent Bragg wavelength shift was observed and measured, and the temperature response as well.

4.2 EXPERIMENT CONFIGURATIONS

In order to measure the strain sensitivity and the temperature sensitivity of a bended fiber Bragg gratin, an experimental configuration is setup as shown in Figure 4-2.

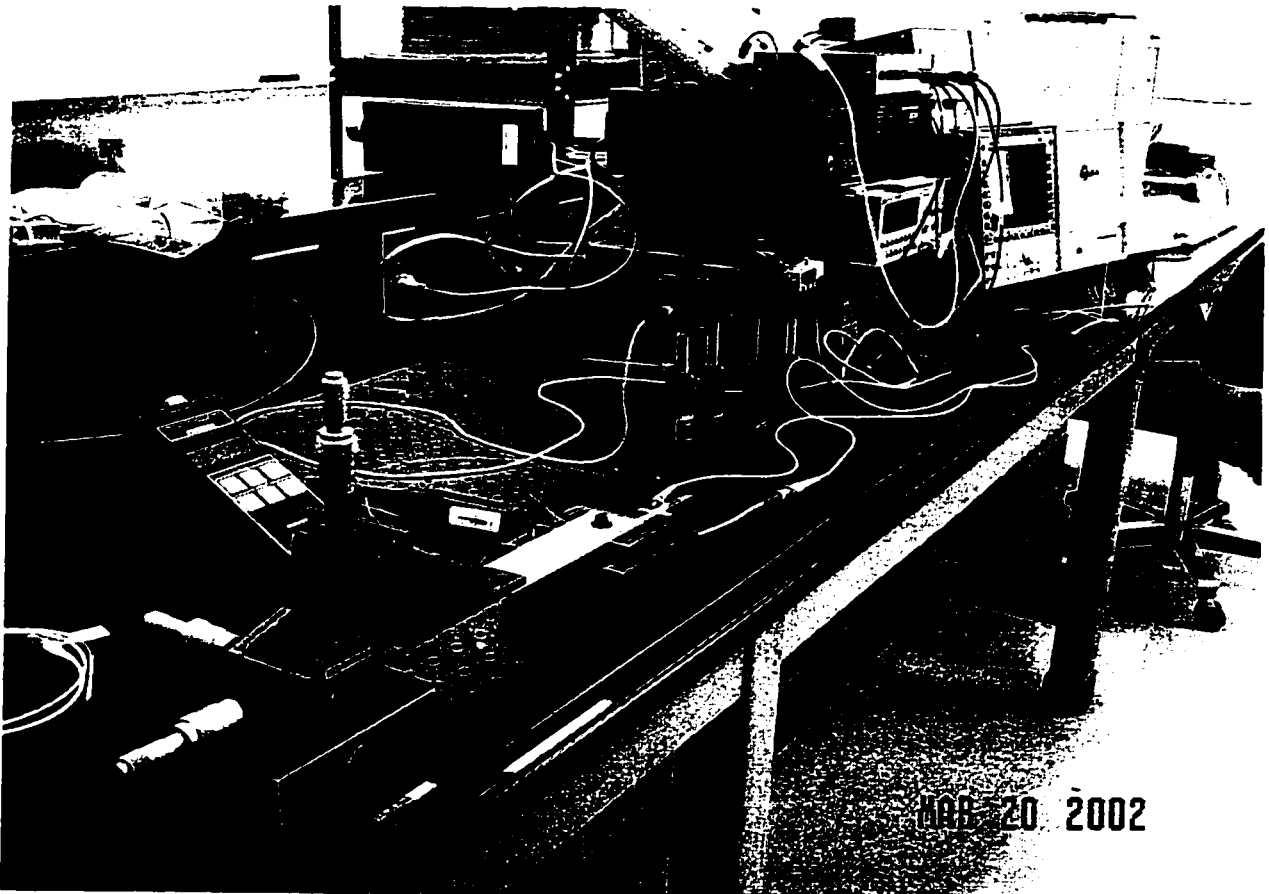


Figure 4-2, Photograph of a global view of the experimental setup

The equipments and components used in this experiment are listed as below:

- Uniform period fiber Bragg grating (made by BRAGG Photonics Inc. Canada)
with specifications:
 - Central Wavelength: 1552.9nm

- FWHM: 0.29nm
- Maximum Reflectivity: 99.9%
- Length: 30mm
- Broadband light source (HP 83437A) with central wavelength at 1550nm
- Optical spectrum analyzer (HP 70952B) with analyzing range from 600 to 1700nm
- Thermometer (Omega HH21) with a K type (NiCr-NiAl) thermocouple
- 50/50 2-by-2 coupler with FC type connectors
- Micrometer
- 45mm×155mm rectangular aluminum beam
- ST-FC adaptor (3dB loss)

The uniform spacing fiber Bragg grating is attached on a rectangular aluminum cantilever beam (Figure 4-3) by using Devcon epoxy, cured at room temperature for 5 minutes. A strain variation is applied on the FBG through the bending of the aluminum cantilever beam. The aluminum beam is bended in such a way that one end is fixed by screwed on a base and the other end is deformed by a micrometer controlled displacing module, so the displacement can be accurately adjusted (Figure 4-4).

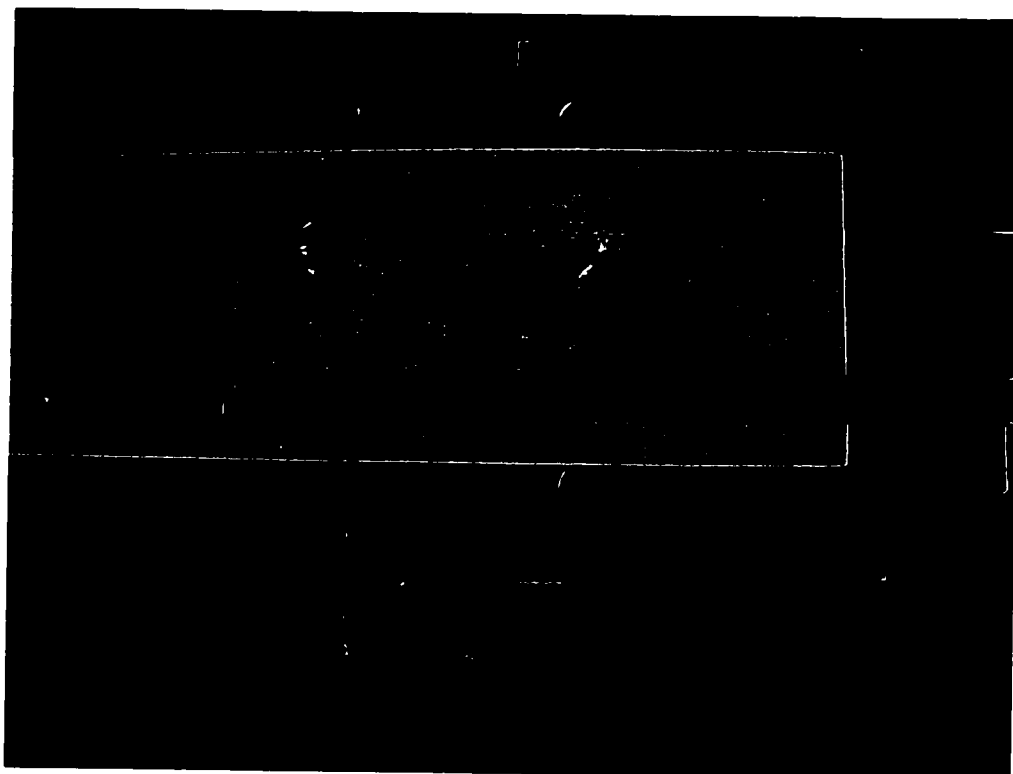


Figure 4-3, Photo of fiber Bragg grating attached cantilever beam

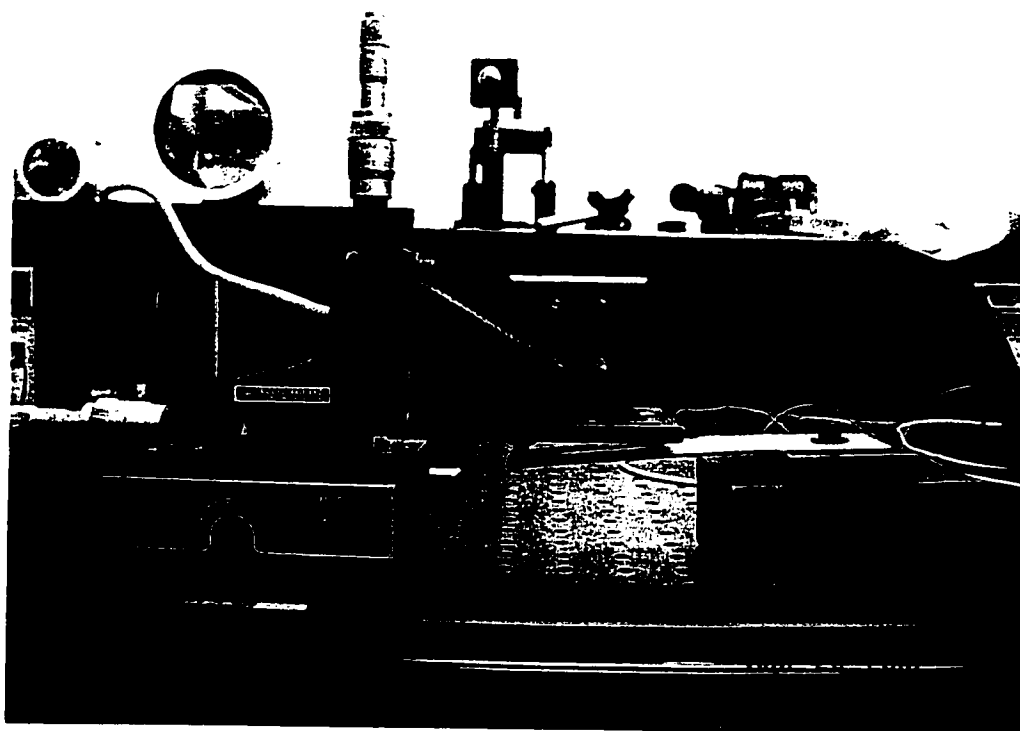


Figure 4-4, Photo of bended cantilever beam

For observing the strain response of the FBG, it is easier to look at the spectrum of the reflected light than the transmission spectrum. A 2×2 coupler is used to guide the reflected light of FBG, so it can be separated from the input light and be measured. A 1550nm broadband edge-emitting LED (EELED) light source is used to provide a light interacting with the FBG. The EELED light source is connected to port 1 of the 2×2 coupler, while the FBG is connected to port 3 and an optical spectrum analyzer is used to measure the reflected spectrum through port 2, as illustrated in Figure 4-5. In order to connect the bare FBG and the cabled 2×2 coupler (with FC connectors), the FBG is fused with a connector (ST type) attached single-mode fiber and then connected to the 2×2 coupler through a ST-FC adapter.

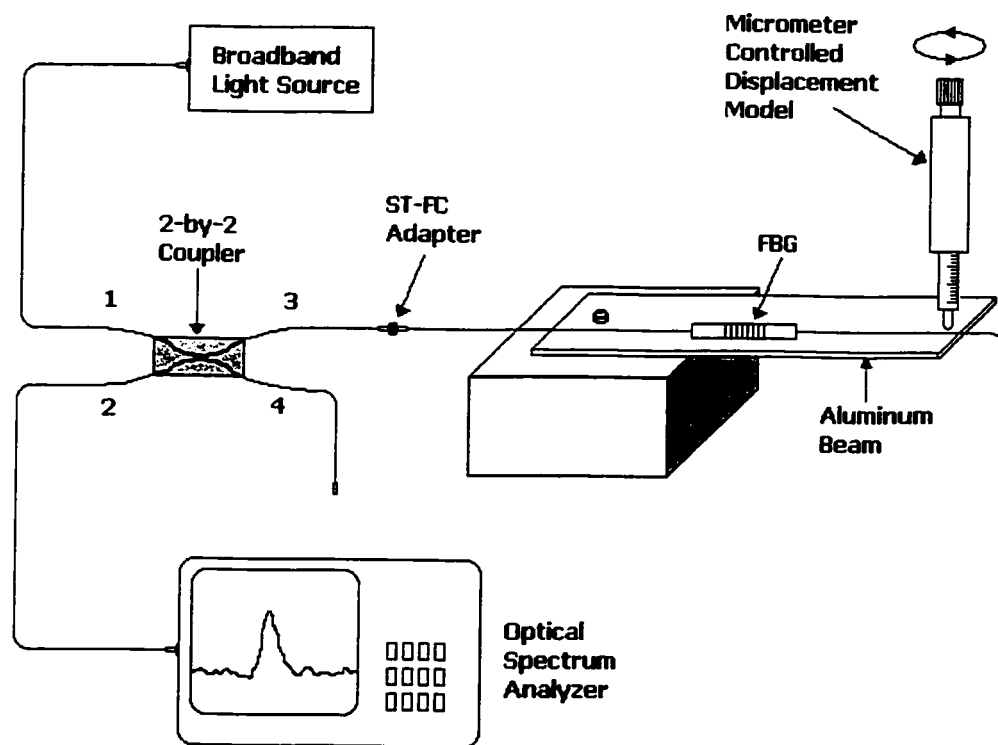


Figure 4-5 Experiment arrangement used for measurement of strain response of fiber Bragg grating

4.3 STRAIN RESPONSE MEASUREMENT

Experimental measurements of the reflected spectra of the bended fiber Bragg grating were taken when the aluminum beam was subjected to static linear displacement. The tip of the aluminum beam was pressed down by the micrometer controlled displacement model. The vertical displacement was increased from 0 to 5mm. Beyond certain point the displacement cannot be increased anymore, because the resistance of the material became greater than the force the displacement model can provide. Although a more powerful displacement gauge can be used here, the limit of linear behavior of the bended material needs to be figured out first. If the material bears a stress greater than its linear limitation, it will be deformed permanently. This should be prevented to keep the system a good tunable ability. When the aluminum beam was deformed, the grating spacing was changed linearly with the linear strain variation. By displacing the beam tip down, the Bragg wavelength is shifted to longer wavelength, and a reverse displacement will results in wavelength shift in the reverse direction, which is to shorter wavelength. Due to the limitation of deflecting device, only one direction was measured. An optical spectrum analyzer (HP70952B) was used to monitor the reflected spectrum. Data is recorded in a PC through a Labview programmed interface controlling parameters of the OSA. Base on the collected data, the reflected spectra of different level of displacement are shown in Figure 4-6. Observing the central reflected wavelength, a linear shift of the central wavelength with the increasing deflection of the beam can be seen. This means the reflected color of light can be adjusted by simply change the level of deflection of the cantilever beam.

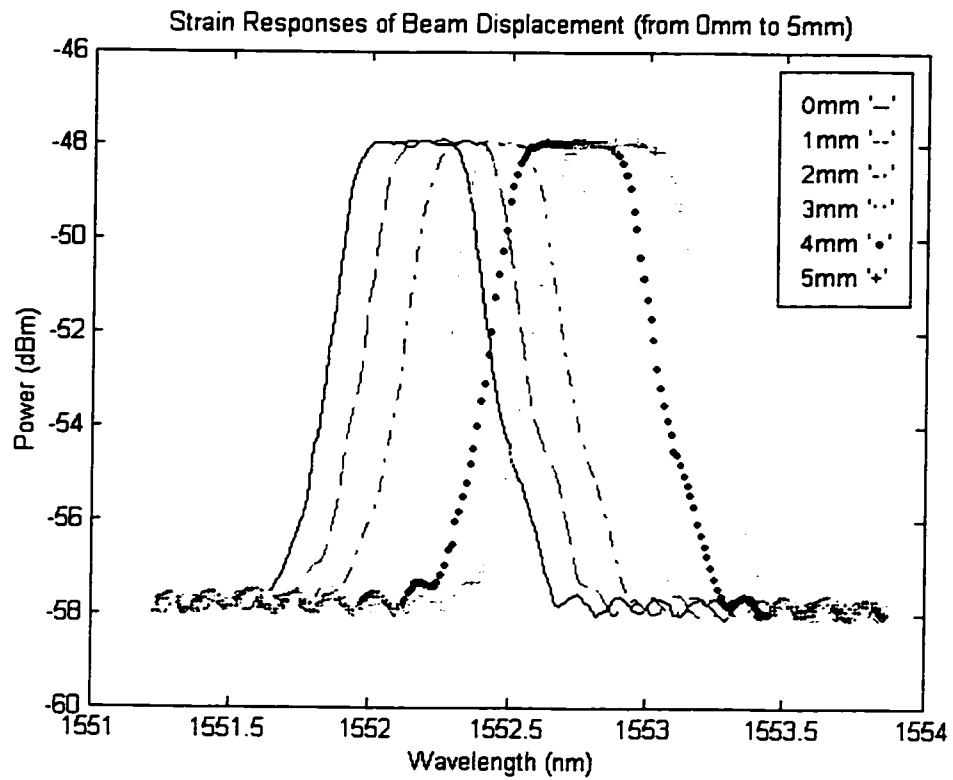


Figure 4-6, Strain response of the FBG at different level of vertical beam displacement

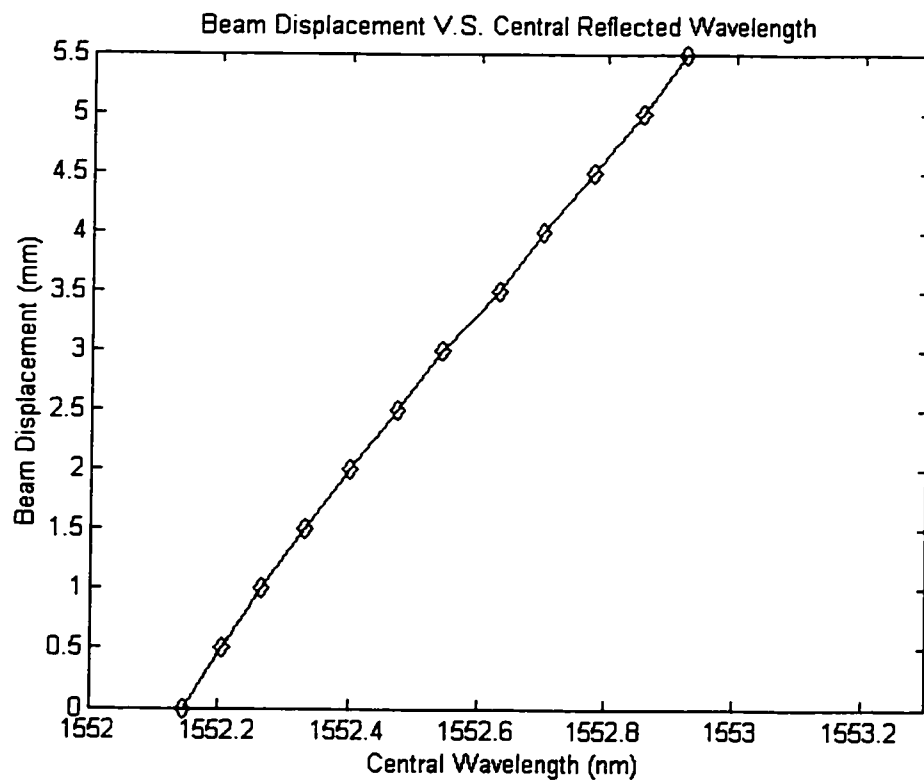


Figure 4-7, Shift of central reflected wavelength due to beam displacement

4.4 TEMPERATURE RESPONSE MEASUREMENT

Since temperature stability of an optical component is always an important parameter, an experiment was setup as shown in Figure 4-8 in order to measure the temperature variation response of the designed module.

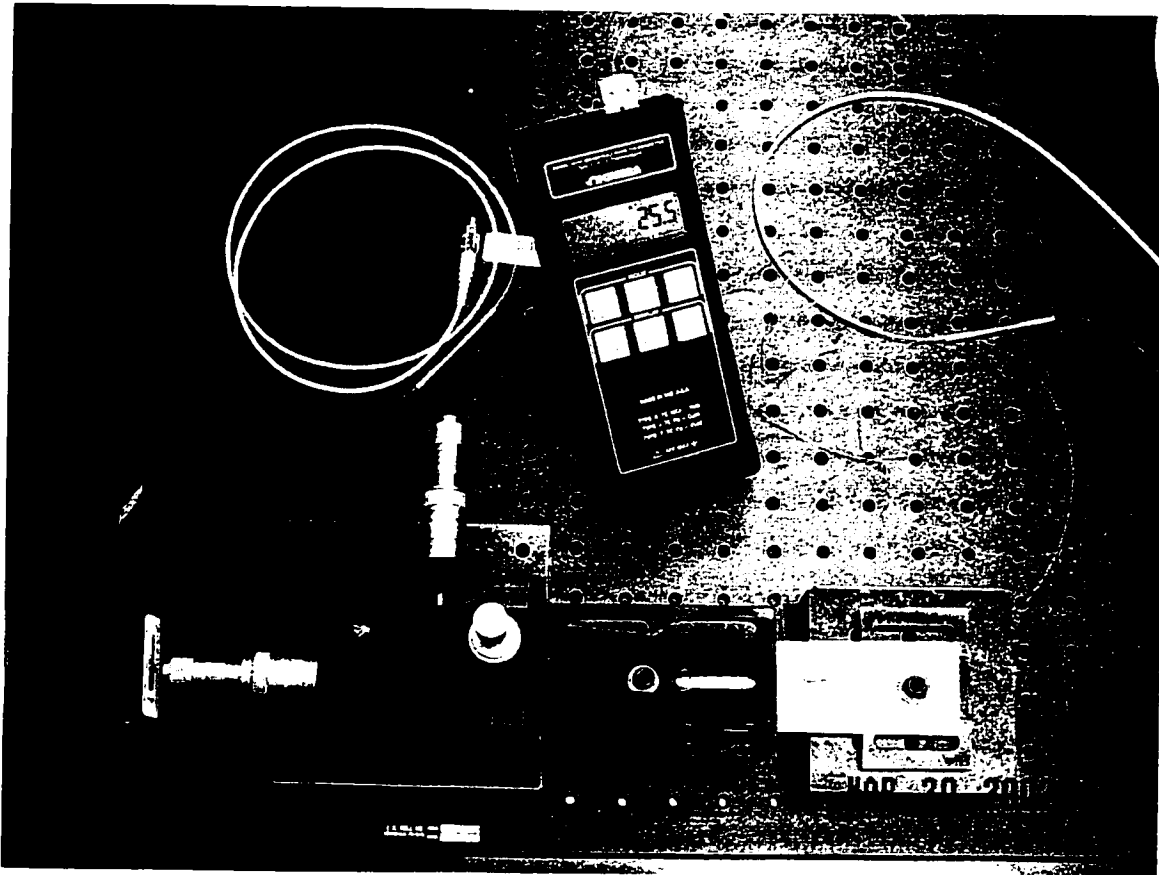


Figure 4-8, Photo of experiment setup for temperature response measurement

The temperature variation of FBG was provided through heating the metal beam by using an oven lighter under the beam. A thermal couple was taped on the beam near the FBG region, and a thermometer was used to read the temperature. The reflected spectra of different temperature were record and plotted as below. The measured temperature induced shift in Bragg wavelength is about $0.03\text{nm}/^{\circ}\text{C}$. The temperature response compared to strain response is much slower, because it takes time to bring the whole

setup including FBG, cantilever beam, and surrounding epoxy to the same temperature uniformly.

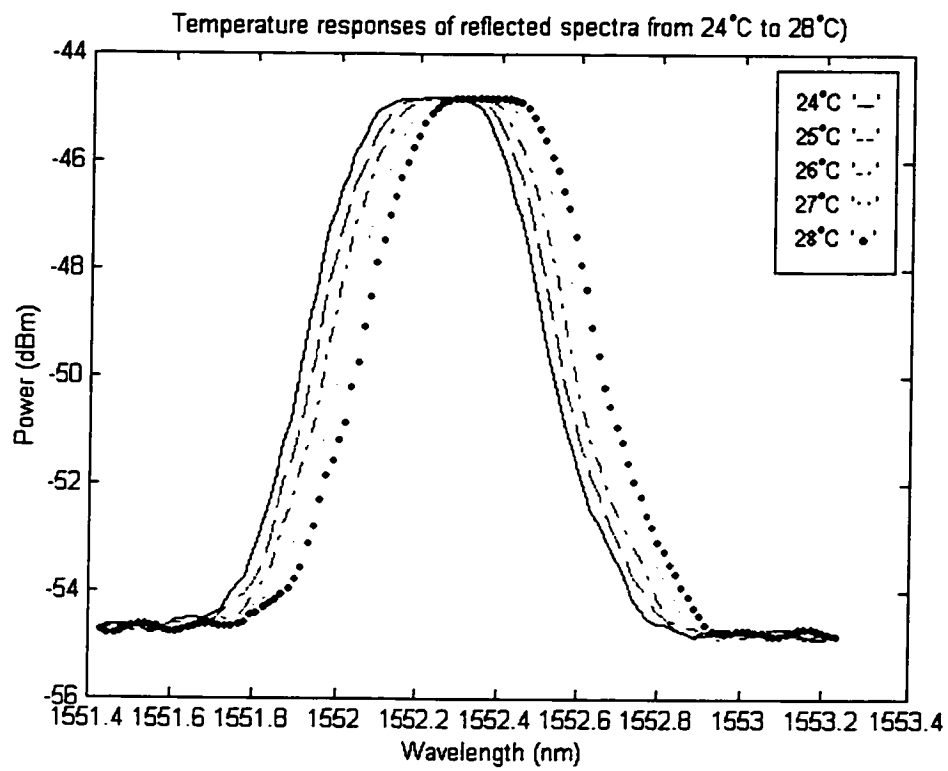


Figure 4-9, Reflected spectra of FBG measured at different temperature

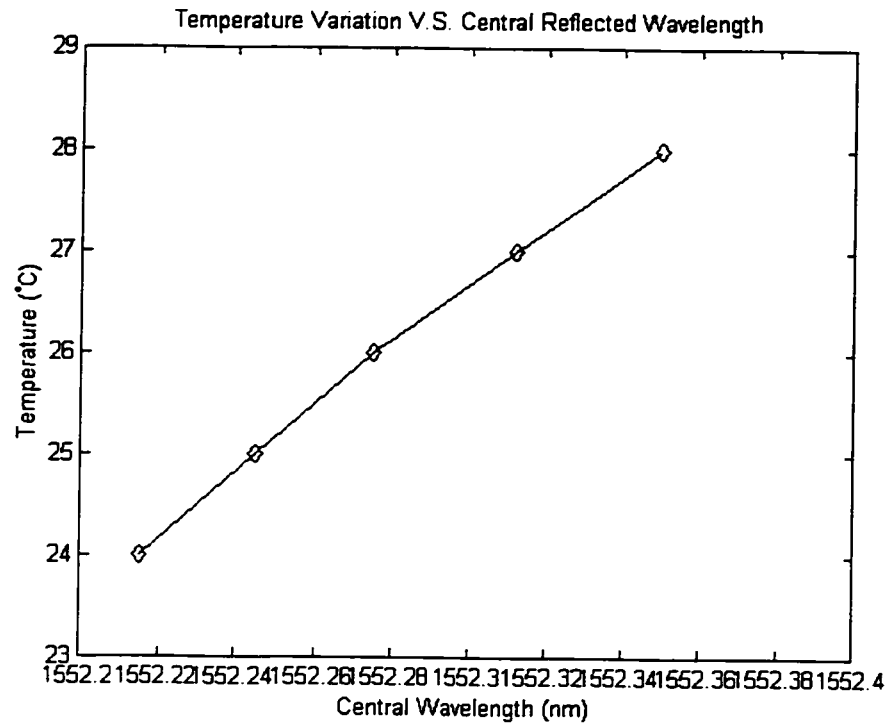


Figure 4-10, Shift of central reflected wavelength due to temperature variation

4.5 SUMMARY

A tunable dispersion-compensating scheme based on bending a FBG attached cantilever beam is demonstrated in this experiment. A linear central wavelength shift of the FBG's reflected spectrum due to deflection level changing of the cantilever beam was measured. A tuning ratio of 0.14nm per millimeter deflection is achievable, and a temperature fluctuation response of 0.03nm/°C is observed.

CHAPTER 5: CONCLUSION

As explained in chapter 1, DWDM technology has tremendously increased the transmission capacity of optical communication systems to meet increasing demand for communication services. It is known power attenuation and chromatic dispersion can degrade an optical pulse resulting unable recovered signal at the receiver end. While using optical amplifiers such as EDFA can compensate the reduced power for long distance link, the chromatic dispersion also needs to be compensated to avoid accumulation of dispersion. In order to transmit more channels in a fiber or increase transmission speed in each channel, dispersion effect must be suppressed. Fiber Bragg gratings have been proved to be a very good choice for providing dispersion compensation for individual channels of DWDM system.

5.1 DISCUSSION OF THE EXPERIMENTAL RESULTS

Attaching a uniform period grating to a cantilever beam and then bending the beam may form a linearly chirped fiber Bragg grating. Such a chirped grating has potential applications in fiber optic communication systems, as dispersion compensators, or in sensing applications. In this paper, a novel dispersion tuning technique was demonstrated, which is based on deflecting a simple aluminum cantilever beam with a uniform spacing fiber Bragg grating mounted on its surface. The strain profile of the beam has been determined by the shape of the metal plate to establish the strain gradient during loading. As a result of the strain gradient, the local Bragg wavelength is a function of the position along the length of the fiber grating so that the grating chirp is an automatic consequence of the strain gradient. This method provides the dynamic control of the Bragg wavelength shift.

Given this flexibility in changing the Bragg grating's wavelength output via simple beam deformation, it is therefore possible to construct a simple wavelength dependent dispersion compensating method. This means each channel of a DWDM system can have its own equalizing filter tuned to the particular value of dispersion seen by the channel. Although the tuning range is restricted in few nanometers, a different wavelength of Bragg grating or different material of cantilever beam can be used to cover different spectrum region. For compensating different amount of dispersion, different length of FBG is required. As a result, establish a flexible manufacturing process will be a necessary to provide this device cost efficiently.

5.2 SUGGESTIONS FOR FUTURE RESEARCH

The system described here is not an optimum system design. For practical implementation, the temperature fluctuation of reflected Bragg wavelength should be prevented from strain controlled wavelength shift in order to obtain an accurate wavelength selecting, therefore, a further research of thermal isolation for fiber Bragg grating is required.

REFERENCES

1. K. C. Kao and G. A. Hockman, "Dielectric Fiber Surface Waveguides for Optical Frequencies," *Proc. IEE*, vol. 133, pp. 1151-1158, July 1966.
2. F. P. Kapron, D. B. Keck, and R. D. Maurer, "Radiation Losses in Glass Optical Waveguides," *Appl. Phys. Lett.*, vol. 17, pp. 423-425, Nov. 1980.
3. C. Lin, "Optical Fiber Transmission Technology," Ch. 1 in *Handbook of Microwave and Optical Components*, Ed. K. Chang, John Wiley, 1991.
4. M. S. Roden, "Analog and Digital Communication Systems," 4th Ed., Prentice Hall, 1996.
5. http://www.cisco.com/univercd/cc/td/doc/product/mels/cm1500/dwdm/dwdm_ovr.htm, "Fundamentals of DWDM Technology," Cisco Inc.
6. T. E. Stern and K. Bala, "Multiwavelength Optical Networks – A Layered Approach," Addison-Wesley, 1999.
7. D. Stoll, P. Leisching, H. Bock, and A. Richter, "Metropolitan DWDM: a dynamically configurable ring for the KomNet field trial in Berlin," *IEEE Communications Magazine*, v39, 2, p 106-113, Feb. 2001.
8. A. F. Wallace, "Ultra long-haul DWDM: Network economics," *Conference on Optical Fiber Communication, Technical Digest Series*, v 54, n 2, 2001.
9. S. V. Kartalopoulos, "Introduction to DWDM Technology: Data in a Rainbow," *IEEE Press*, Piscataway, NJ, 2000.
10. J. Senior, "Optical Fiber Communications: Principles and Practice," Prentice Hall, Englewood Cliffs, NJ, 1985.
11. B. Mukherjee, "Optical Communication Networks," McGraw-Hill, 1997.
12. M. M. Liu, "Principles and Applications of Optical Communications," Irwin, 1996.
13. J. C. Palais, "Fiber Optic Communications," 4th Ed., chapter 6, Prentice-Hall, Upper Saddle River, NJ, 1998.
14. G. Keiser, "Optical Fiber Communications," 2nd Ed., chapter 4, McGraw Hill, 1991.

15. C. A. Burrus and B. J. Miller, "Small-area, Double Heterostructure AlGaAs Electro-luminescent Diode Sources for Optical-Fiber Transmission Lines," *Optical Communications*, vol. 4, Elsevier Science Publishers, pp. 307-309, 1971.
16. R. H. Saul, T. P. Lee, and C. A. Burrus, "Light-Emitting-Diode Device Design," Chapter 5, *Lightwave Communications Technology, Part C*, edited by W. T. Tsang, Semiconductors and Semimetals, vol. 22, Academic Press, 1985.
17. B. Schwartz et al., "Stripe Geometry InP/InGaAsP Lasers Fabricated with Deuteron Bombardment," *IEEE Transactions on Electron Devices*, vol. 31, pp. 841-843, 1984.
18. K. Oe and K. Sugiyama, "GaInAsP/InP Planar Stripe Lasers Prepared by Using Sputtered SiO₂ Film as a Zn Diffusion Mask," *Journal of Applied Physics*, vol. 51, no. 1, pp. 43-49, 1980.
19. T. P. Lee, C. A. Burrus, R. A. Linke, and R. J. Nelson, "Short-cavity, single-frequency InGaAsP buried heterostructure lasers," *Electron. Lett.*, vol. 19, pp. 82-84, Feb. 1983.
20. K. Kobayashi and I. Mito, "Single frequency and tunable laser diodes," *Journal of Lightwave Technology*, vol. 6, no. 2, pp. 1623-1633, Nov. 1988.
21. C. J. Koester and E. Snitzer, "Amplification in a Fiber Laser," *Applied Optics*, vol. 3, pp. 1182, 1964.
22. W.J. Miniscalco, "Erbium-Doped Glasses for Fiber Amplifiers at 1500nm," *Journal of Lightwave Technology*, vol. 9 no. 2, pp.234-250, Feb. 1991.
23. S. R. Forrest, "Optical Detectors for Lightwave Communication," Chapter 14 of *Optical Fiber Telecommunications II*, edited by S.E. Miller and I. P. Kaminow, Academic Press, 1988.
24. S. R. Forrest, "Optical detectors: Three contenders," *IEEE Spectrum*, vol. 23, pp. 76-84, May 1986.
25. P. P. Webb, R. J. McIntyre, and J. Conradi, "Properties of avalanche photodiodes," *RCA Review*, vol. 35, pp. 234-278, June 1974.
26. J. E. Bowers and C. A. Burrus, "Ultrawide-band long-wavelength p-i-n photodetectors," *J. Lightwave Tech.*, vol. LT-5, pp. 1339-1350, Oct. 1987.
27. J. N. Hollenhorst, "Fabrication and performance of high-speed InGaAs APDs," *Tech Digest OSA/IEEE Opt. Fiber Comm. Conf.*, p.148, Jan. 1990.

28. T. P. Lee and T. Li, "Photodetectors," in *Optical Fiber Telecommunications*, edited by S. E. Miller and A. C. Chynoweth, Academic, New York, 1979.
29. J. E. Midwinter, "Optical Fibers for Transmission," New York, John Wiley, pp.128-161, 1979.
30. B. C. Bagley, C. R. Kurkjian, J. W. Mitchell, G. E. Peterson, and A. R. Tynes, "Materials, properties, and choices," in *Optical Fiber Telecommunications*, edited by S. E. Miller and A. C. Chynoweth, Academic, New York, 1979.
31. R. Olshansky, "Propagation in glass optical waveguides," *Rev. Mod. Phys.*, vol. 51, pp.341-367, Apr. 1979.
32. D. Gloge, "The optical fiber as a transmission medium," *Rpts. Prog. Phys.*, vol. 42, pp. 1777-1824, Nov. 1979.
33. H. Osanai, T. Shioda, T. Moriyama, S. Araki, M. Horiguchi, T. Izawa, and H. Takara, "Effects of dopants on transmission loss of low-OH-content optical fibers," *Electronics Letters*, 12, no. 21, Oct. 1976.
34. T. Moriyama, O. Fukuda, K. Sanada, K. Inada, T. Edahiro, and K. Chida, "Ultimately low OH content VAD optical fibers," *Electron Lett.*, vol. 16, pp. 699-700, Aug. 1980.
35. D. Gloge, "Dispersion in weakly guiding fibers," *Applied Optical*, vol. 10, pp. 2442-2445, 1971.
36. J. C. Palais, "Fiber Optic Communications," 4th Ed., Chapter 5, Prentice-Hall, Upper Saddle River, NJ, 1998.
37. J. M. Senior, "Optical Fiber Communications: Principles and Practice," 2nd ed., Prentice-Hall International (UK), 1992.
38. S. C. Mettler and C. M. Miller, "Optical Fiber Splicing," chapter 6 of *Optical Fiber Telecommunications II*, edited by S. E. Miller and I. P. Kaminow, Academic Press, 1988.
39. W. Goralski, "Optical Networking & WDM," McGraw-Hill, 2001.
40. M. Y. El-Ibiary, "Parameter optimization in graded-index dispersion-shifted single-mode fibers," *J. Lightwave Tech.*, vol. LT-4, pp. 364-367, Mar. 1986.
41. W. A. Reed, L. G. Cohen, and H. T. Shang, "Tailoring optical characteristics of dispersion-shifted lightguides for applications near 1.55 μm ," *AT&T Tech. J.*, vol. 65, pp.105-122, Sept./Oct. 1986.

42. D. Kalish and L. G. Cohen, "Single-mode fiber: From research and development to manufacturing," *AT&T Tech. J.*, vol. 66, pp.19-32, Jan./Feb. 1987.
43. T. D. Croft, J. E. Ritter, and V. A. Bhagavatula, "Low-loss dispersion-shifted single-mode fiber manufactured by OVD process," *J. Lightwave Tech.*, vol. LT-5, pp. 931-934, Oct. 1985.
44. G. Keiser, "Optical Fiber Communications," 2nd Ed., chapter 3, McGraw Hill, 1991.
45. M. A. Saifi and S. J. Jang, "Triangular-Profile Single-Mode Fiber," *Opt. Lett.*, vol. 7, pp.43-45, Jan. 1982.
46. Y. Nagasawa, K. Aikawa, N. Shamoto, A. Wada, Y. Sugimasa, I. Suzuki, and Y. Kikuchi, "High performance dispersion compensating fiber module," Fujikura Technical Review No.30, Jan. 2001.
47. D. C. Flanders, H. Kogelnik, R. V. Schmidt, and C. V. Shank, "Grating filters for thin-film optical waveguides," *Applied Physics Letters*, 24, pp. 194-196, 1974.
48. R. Measures, T. Alavie, S. Karr and T. Coroy, "Smart structure interface issues and their resolution: Bragg grating laser sensor and the optical synapse," *Proc. SPIE*, vol. 1918, 1993.
49. D. B. Hunter and R. A. Minasian, "Tunable microwave fiber-optic bandpass filters," *IEEE Photonics Technology Letters*, v 11, n 7, pp.874-876, 1999.
50. D. Sadot and E. Boimovich, "Tunable optical filters for dense WDM networks," *IEEE Comm. Mag.*, v 36, n 12, pp. 50-55, Dec. 1998.
51. F. Bilodeau, K. O. Hill, B. Malo, D. C. Johnson, and J. Albert, "High-return-loss narrowband all-fiber bandpass Bragg transmission filter," *IEEE Photonics Tech. Lett.*, v 6, n 1, pp. 80-82, Jan. 1994.
52. W. Morey, G. Meltz and W. Glenn, "Fiber optic Bragg grating sensors," *Proc. SPIE*, vol. 1169, pp. 98-107, 1989.
53. J. Dunphy, G. Meltz and W. Morey, "Optical fiber Bragg grating sensors: A candidate for smart structure applications," Ch. 10 in *Fiber Optic Smart Structures*, Ed. E. Udd, John Wiley, 1995.
54. J. Martin and F. Ouellette, 'Novel writing technique of long and highly reflective in-fiber gratings,' *Electron. Lett.*, vol. 30, pp. 811-812, 1994.

55. P. L. Fuhr, D. R. Huston, and A. McPadden, "Non-Contact Deflection Measurements in Structures Using Diffraction Gratings," Proceedings of the ACI Convention, Montreal, Quebec, Canada, Nov. 1995.
56. K. O. Hill, Y. Fujii, D. C. Johnson, and B. S. Kawasaki, "Photosensitivity in optical fiber waveguides: Application to reflection filter fabrication," *Appl. Phys. Lett.*, vol. 32, pp. 647-649, 1978.
57. B. S. Kawasaki, K. O. Hill, D. C. Johnson, and Y. Fujii, "Narrow-band Bragg reflectors in optical fibers," *Opt. Lett.*, vol. 3, pp. 66-68, 1978.
58. G. Meltz, W. W. Morey, and W.H.Glenn, "Formation of Bragg gratings in optical fibers by a transverse holographic method," *Opt. Lett.*, vol. 14, pp. 823-825, 1989.
59. D. K. W. Lam and B. K. Garside, "Characterization of single-mode optical fiber filters," *Appl. Opt.*, vol. 20, pp. 440-445, 1981.
60. Y. Painchaud, A. Chandonnet, and J. Lauzon, "Chirped fiber gratings produced by tilting the fiber," *Electron. Lett.*, vol. 31, pp. 171-172, 1995.
61. K. C. Byron and H. N. Rourke, "Fabrication of chirped fiber gratings by novel stretch and write technique," *Electron. Lett.*, vol. 31, pp. 60-61, 1995.
62. L. Dong, J. L. Cruz, L. Reekie, and J. L. Archambault, "Tuning and chirping fiber Bragg gratings by deep etching," *IEEE Photon. Technol. Lett.*, vol. 7, pp. 1433-1435, 1995.
63. R. Kashyap, P. F. McKee, R. J. Campbell, and D. L. Williams, "Novel method of producing all fiber photoinduced chirped gratings," *Electron. Lett.*, vol. 30, pp. 996-997, 1994.
64. F. Quellette, "Dispersion cancellation using linearly chirped Bragg grating filters in optical waveguides," *Opt. Lett.*, vol. 12, pp. 847-849, 1987.
65. J. C. Palais, "Fiber Optic Communications," 4th Ed., chapter 3, Prentice-Hall, Upper Saddle River, NJ, 1998.
66. F. Quellette, J. F. Cliché, and S. Gagnon, "All-fiber devices for chromatic dispersion compensation based on chirped distributed resonant coupling," *Journal of Lightwave Technology*, vol. 12, no. 10, pp. 1728-1737, Oct. 1994.
67. P. C. Hill and B. J. Eggleton, "Strain gradient chirp of fiber Bragg grating," *Electron. Lett.*, vol. 30, pp. 1172-1174, 1994.

68. M. M. Ohn, A. T. Alavie, R. Maaskant, M. G. Xu, F. Bilodeau, and K. O. Hill, "Dispersion variable fiber grating using a piezoelectric stack," *Electron. Lett.*, vol. 32, pp. 2000-2001, 1996.
69. M. Pacheco, A. Medez, L. A. Zenteni, and F. Mendoz-Santoyo, "Chirping optical fiber Bragg gratings using tapered-thickness piezoelectric ceramic," *Electron. Lett.*, vol. 34, pp. 2348-2350, 1998.
70. J. Lauzon, S. Thibault, J. Martin, and F. Quелlette, "Implementation and characterization of fiber Bragg gratings linearly chirped by a temperature-gradient," *Opt. Lett.*, vol. 19, pp. 2027-2029, 1994.
71. S. Barcelos, M. N. Zervas, R. I. Laming, D. N. Payne, L. Reekie, J. A. Tucknott, R. Kashyap, P. F. MaKee, F. Sladen, and B. Wojciechowicz, "High-accuracy dispersion measurements of chirped fiber gratings," *Electron. Lett.*, vol. 31, pp. 1280, 1995.
72. T. Eftimov, M. C. Farries, S. Huang, N. Duricic, D. Grobnic, B. Keyworth, and J. S. Obhi, "8-channel tunable drop device with thermal tuning for 100 GHz channel spacing," in Proc. ECOC'98, Madrid, Spain, pp.127-128, 1998.
73. B. J. Eggleton, J. A. Rogers, P. S. Westbrook, and T. A. Strasser, "Electrically tunable power efficient dispersion compensating fiber Bragg grating," *IEEE Photo. Tech. Lett.*, vol. 11, no. 7, pp. 854-856, 1999.
74. A. D. Kersey, M. A. Davis, H. J. Patrick, M. LeBlanc, K. P. Koo, C. G. Askins, M. A. Putnam, and E. J. Friebele, "Fiber grating sensors," *Journal of Lightwave Tech.*, Vol. 15, No. 8, pp. 1442-1462, Aug. 1997.
75. W. Morey, J. Dunphy, and G. Meltz, "Multiplexed fiber Bragg grating sensors," Proc. SPIE 1586, pp. 216-224, 1991.
76. T. N. Nielsen, B. J. Eggleton, J. A. Rogers, P. S. Westbrook, P. B. Hansen, and T. A. Strasser, "Dynamic post dispersion optimization at 40 Gb/s using a tunable fiber Bragg grating," *IEEE Photo. Tech. Lett.*, vol. 12, no. 2, pp. 173-175, Feb. 2000.
77. B. J. Eggleton, B. Mikkelsen, G. Raybon, A. Ahuja, J. A. Rogers, P. S. Westbrook, T. N. Nielsen, S. Stulz, and K. Dreyer, "Tunable dispersion compensation in a 160-Gb/s TDM system by a voltage controlled chirped fiber Bragg grating," *IEEE Photo. Tech. Lett.*, vol. 12, no. 8, pp. 1022-1024, Aug. 2000.
78. K. L. Hill, F. Bilodeau, B. Molo, T. Kitagawa, S. Theriault, D. C. Johnson, and J. Albert, "Chirped in-fiber Bragg gratings for compensation of optical-fiber dispersion," *Opt. Lett.*, vol. 19, pp. 1314-1316, 1994.

79. K. H. Huebner, "The finite element method for engineers," John Wiley & Sons, Inc., N.Y., 1975